Plant Physiology®

Plant Physiology, 2025, **197**, kiae575
https://doi.org/10.1093/plphys/kiae575
Advance access publication 29 October 2024
Research Article

Mitogen-activated protein kinase 4 phosphorylates MYC2 transcription factors to regulate jasmonic acid signaling and herbivory responses in maize

Sen Li,[1,2] Canrong Ma,[1,2] Shalan Li,[3] Mou Zhang,[1,2] Cuiping Zhang,[1,2] Jinfeng Qi,[1,2,4] Lei Wang,[1,2,4] Xuna Wu,[3] Jing Li,[1,2,*] Jianqiang Wu[1,2,4,*]

[1]Department of Economic Plants and Biotechnology, Yunnan Key Laboratory for Wild Plant Resources, Kunming Institute of Botany, Chinese Academy of Sciences, Kunming 650201, China
[2]CAS Center for Excellence in Biotic Interactions, University of Chinese Academy of Sciences, Beijing 100049, China
[3]State Key Laboratory of Conservation and Utilization of Bio-Resources in Yunnan and Center for Life Science, School of Life Science, Yunnan University, Kunming 650500, China
[4]State Key Laboratory of Plant Diversity and Prominent Crops, Beijing 100093, China
*Author for correspondence: lijing1@mail.kib.ac.cn (J.L.), wujianqiang@mail.kib.ac.cn (J.W.)
The author responsible for distribution of materials integral to the findings presented in this article in accordance with the policy described in the Instructions for Authors (https://academic.oup.com/plphys/pages/General-Instructions) is: Jianqiang Wu (wujianqiang@mail.kib.ac.cn).

Abstract

Regulation of responses induced by herbivory and jasmonic acid (JA) remains poorly understood in the important staple crop maize (*Zea mays*). MYC2 is the key transcription factor regulating many aspects of JA signaling, while mitogen-activated protein kinases (MAPKs or MPKs) play important roles in various plant physiological processes. Using a combination of reverse genetics, transcriptome analysis, and biochemical assays, we elucidated the important role of mitogen-activated protein kinase 4 (MPK4) in maize resistance to insects and in JA signaling. Silencing *MPK4* increased the JA and jasmonoyl-isoleucine levels elicited by wounding or simulated herbivory but decreased maize resistance to armyworm (*Mythimna separata*) larvae. We showed that MPK4 is required for transcriptional regulation of many genes responsive to methyl jasmonate, indicating the important role of maize MPK4 in JA signaling. Biochemical analyses indicated that MPK4 directly phosphorylates MYC2s at Thr115 of MYC2a and Thr112 of MYC2b. Compared with nonphosphorylated MYC2s, phosphorylated MYC2s were more prone to degradation and exhibited enhanced transactivation activity against the promoters of several benzoxazinoid biosynthesis genes, which are important for maize defense against insects. This study reveals the essential role of maize MPK4 in JA signaling and provides insights into the functions of MAPKs in maize.

Introduction

Plants are constantly challenged by abiotic and biotic stresses, including insect herbivory. Accordingly, plants have evolved sophisticated strategies to defend against insects. Upon wounding or insect herbivory, plants perceive stimuli by sensing damage- and/or herbivore-associated molecular patterns and thereby initiate a broad range of early defense responses, including depolarization of the membrane potential, influxes of Ca^{2+}, activation of mitogen-activated protein kinases (MAPKs), production of reactive oxygen species, and induction of jasmonates (Erb and Reymond 2019). Among these, jasmonic acid (JA) and its bioactive derivative jasmonoyl-isoleucine (JA-Ile) have long been established as the critical regulators in plant defense responses against insects (Staswick and Tiryaki 2004; Fonseca et al. 2009; Erb and Reymond 2019). Many lines of evidence have demonstrated that the JA pathway controls accumulation of plant defensive secondary metabolites, which are toxic or deterrent to the herbivores or attractive to the predators or parasitoids of the herbivores (War et al. 2012; Divekar et al. 2022).

Upon insect herbivory, JA and the bioactive JA-Ile rapidly accumulate, and JA-Ile promotes the interaction between the receptor COI1 (an E3 ubiquitin ligase) and jasmonate ZIM-domain (JAZ) proteins and thus triggering degradation of JAZ proteins by the 26S proteasome (Chini et al. 2007; Thines et al. 2007; Sheard et al. 2010). JAZs normally form a complex with MYC2, the master transcription factor of JA signaling, and degradation of JAZs releases MYC2, thus activating many of the jasmonate-induced genes (Chini et al. 2007; Thines et al. 2007), including biosynthetic genes of defensive metabolites (De Geyter et al. 2012; Kazan and Manners 2013). Recent evidence has revealed that MYC2 is subjected to multiple posttranslational modifications, and these posttranslational modifications change the activity and/or stability of MYC2 (Yi and Shan 2023). The kinase FERONIA phosphorylates MYC2, leading to degradation of MYC2 (Guo et al. 2018). Arabidopsis casein kinase II also directly phosphorylates MYC2 and thus enhances the binding activity of MYC2 to the promoters of JA-responsive genes (Zhu et al. 2023). Importantly, phosphorylation of Arabidopsis MYC2 leads to its degradation by 26S proteosome (Zhai et al. 2013). It has been reported that the E3 ubiquitin ligase PUB10 targets MYC2 for proteasomal degradation (Jung et al. 2015), and MYC2 and its homologs MYC3 and MYC4 are also negatively modulated by the BTB/POZ-MATH proteins, which

Received May 30, 2024. Accepted September 22, 2024.

function as adaptors of CUL3-based E3 ubiquitin ligases (Chico et al. 2020). MYC2 protein level is also positively regulated by 2 deubiquitinating enzymes UBP12 and UBP13 (Jeong et al. 2017). Moreover, SUMOylation of MYC2 by the SUMO proteases SPF1 and SPF2 promotes its binding to DNA *cis*-elements (Srivastava et al. 2022).

MAPK cascade is an evolutionarily conserved signaling transduction module in eukaryotes, which plays central roles in the transduction of external signals to intracellular responses (Rodriguez et al. 2010; Meng and Zhang 2013). A large body of evidence has demonstrated that 3 MAPKs in Arabidopsis MPK3, MPK4, and MPK6 play important roles in the regulation of plant growth and development and adaptation to environmental stresses, including herbivory (Zhang and Zhang 2022). In rice, OsMPK3 is essential for striped stem borer (*Chilo suppressalis*) feeding-induced JA and trypsin protease inhibitors, and silencing *OsMPK3* compromises the resistance of rice to *C. suppressalis* (Wang et al. 2013). Studies in the wild tobacco (*Nicotiana attenuata*) revealed that wounding-induced protein kinase (WIPK) and salicylic acid (SA)–induced protein kinase (SIPK), which are respectively the orthologs of MPK3 and MPK6 in Arabidopsis, and MPK4 are involved in plant–insect interactions (Wu et al. 2007; Hettenhausen et al. 2013): SIPK and WIPK both control wounding and simulated tobacco hornworm (*Manduca sexta*) herbivory-induced JA and JA-Ile levels and the expression of insect resistance-related genes; MPK4 suppresses the resistance of *N. attenuata* to *M. sexta* in a JA-independent manner. Zhang et al. (2021) reported that silencing maize *MPK6* led to decreased levels of simulated *Mythimna separata* feeding-induced ethylene, and the *MPK6*-silenced maize exhibited increased susceptibility to *Spodoptera litura*, *M. separata*, and *Ostrinia nubilalis*.

Maize is an important cereal crop around the world, whose production is severely threatened by insects (Deutsch et al. 2018; Savary et al. 2019). Like various other species, in response to insect feeding, JA and JA-Ile levels are rapidly elevated in maize (Qi et al. 2016; Tzin et al. 2017), and the JA pathway also plays a critical role in maize resistance to insects. The maize *opr7 opr8* double mutants have dramatically reduced JA and exhibited increased susceptibility to beet armyworm (*S. exigua*; Yan et al. 2012). Loss-of-function mutation of maize *LOX10*, which is involved in JA biosynthesis, led to compromised resistance to *S. exigua* (Christensen et al. 2013). The maize genome harbors 2 *MYC2s*, *MYC2a* and *MYC2b*, and these 2 maize MYC2s have been identified as the important regulators of benzoxazinoids (Bxs), by directly binding and thus activating the promoters of some of the Bx biosynthesis genes and by regulating other transcription factors; the maize *myc2ab* mutants exhibited highly increased susceptibility to the insects *S. frugiperda* and *M. separata* (Ma et al. 2023).

Bxs are a class of important secondary metabolites in the Poaceae family including maize (Niemeyer 2009). In maize, Bxs are synthesized by a near linear series of enzymes. Indole-3-glycerol phosphate is converted into indole by BX1 (Richter et al. 2021), and indole is further transformed by a series of enzymes (BXs, BX2 to BX9) to DIMBOA-Glc (Frey et al. 2009), which can be further catalyzed by BX10, BX11, BX12, and BX14 to form HDMBOA-Glc (Meihls et al. 2013) or converted to be DIM2BOA-Glc by BX13, and DIM2BOA-Glc can be further O-methylated by BX14 to form HDM2BOA-Glc (Handrick et al. 2016). Genetic analyses using maize *bx1* or *bx2* mutants, which almost completely lack of Bxs, indicated that Bxs are important for maize resistance to insects (Betsiashvili et al. 2015; Tzin et al. 2015, 2017). Among these Bxs, DIMBOA, DIMBOA-Glc, and HDMBOA-Glc were isolated, and feeding assays revealed that they are toxic to caterpillars (Wouters et al. 2016). The biosynthesis genes of Bxs, *BX1* to *BX14*, are transcriptionally regulated by at least the JA and SA signaling pathways (Ma et al. 2023; Setotaw et al. 2024). In addition to phytohormone signaling, transcriptome analysis indicated that insect feeding, e.g. caterpillars and aphids, activates genome-wide rearrangement of gene expression in maize. For example, treating maize with simulated *M. separata* herbivory resulted in more than 3,000 differentially expressed genes (DEGs; Qi et al. 2016). Similarly, *S. exigua* caterpillar feeding on maize induced more than 2,000 DEGs (Tzin et al. 2017).

Previously, it has been shown that MPK6 is involved in maize defense against insects (Zhang et al. 2021). However, the functions of MPK3 and MPK4 in maize–insect interactions have not been studied. Previous bioinformatic analysis identified a single *MPK4* gene (*Zm00001d047349*) in maize (Liu et al. 2013), which was also named as the salt-induced mitogen-activated protein kinase 1 (*ZmSIMK1*), and ectopically expressing *ZmSIMK1*in Arabidopsis enhanced plant tolerance to salt stress (Gu et al. 2010). Here, we show that silencing *MPK4* in maize resulted in decreased resistance to lepidopteran insects. RNA-Seq analysis revealed that more than 50% of methyl jasmonate (MeJA)-responsive genes were affected by silencing of *MPK4*, indicating that MPK4 is important for the JA signaling. Using biochemical and genetic tools, we show that maize MPK4 plays dual roles: first, MPK4 is required for simulated herbivory- or JA-induced transcriptional responses, including defenses; second, MPK4 directly phosphorylates and destabilizes MYC2s. This study provides insight into the mechanism underlying JA signaling and reveals the essential role of MPK4 in herbivory- and JA-induced responses in maize.

Results

Silencing *MPK4* in maize results in decreased lengths of maize internodes at juvenile stage

Using the amino acid sequence of Arabidopsis MPK4 (AT4G01370) as the search query to BLAST against the maize genome database (https://www.maizegdb.org/), we found that one candidate (Zm00001d047349) has the highest amino acid sequence similarly to Arabidopsis MPK4, and phylogeny analysis also indicated that *Zm00001d047349* is the Arabidopsis *MPK4* ortholog in maize (Supplementary Fig. S1A). To examine the tissue specificity of *MPK4* expression, we analyzed the relative transcriptional abundance of *MPK4* across 6 different tissue types using reverse transcription quantitative PCR (RT-qPCR). *MPK4* mRNA was expressed in maize root, stem, leaf, sheath, tassel, and silk under the normal growth conditions, and among these tissues, root and silk respectively showed the highest and lowest levels of *MPK4* transcripts (5-fold difference; Supplementary Fig. S1B). Furthermore, we examined the subcellular localization of MPK4 by transiently expressing the enhanced GFP (eGFP)–tagged MPK4 in maize protoplasts. MPK4 was found to be localized in the cytoplasm and nucleus (Supplementary Fig. S1C), a result that is consistent with previous studies of MPK4 in Arabidopsis and tobacco (*N. attenuata*; Andreasson et al. 2005; Hettenhausen et al. 2012).

To study the function of MPK4, 2 homozygous transgenic lines irMPK4 #1 and irMPK4 #2 were selected, in which *MPK4* was silenced using RNA interference (RNAi). RT-qPCR analysis showed that the transcriptional levels of *MPK4* were reduced in irMPK4 transgenic lines, reaching about 20% to 30% of the *MPK4* levels in the wild-type (WT) maize (Supplementary Fig. S1D). Furthermore, to rule out the possibility of off-target silencing of *MPK3* and *MPK6*, we examined the expression of *MPK3* and *MPK6* in the WT and irMPK4 lines, and RT-qPCR analysis indicated that *MPK3* and *MPK6* were not silenced in the irMPK4 lines

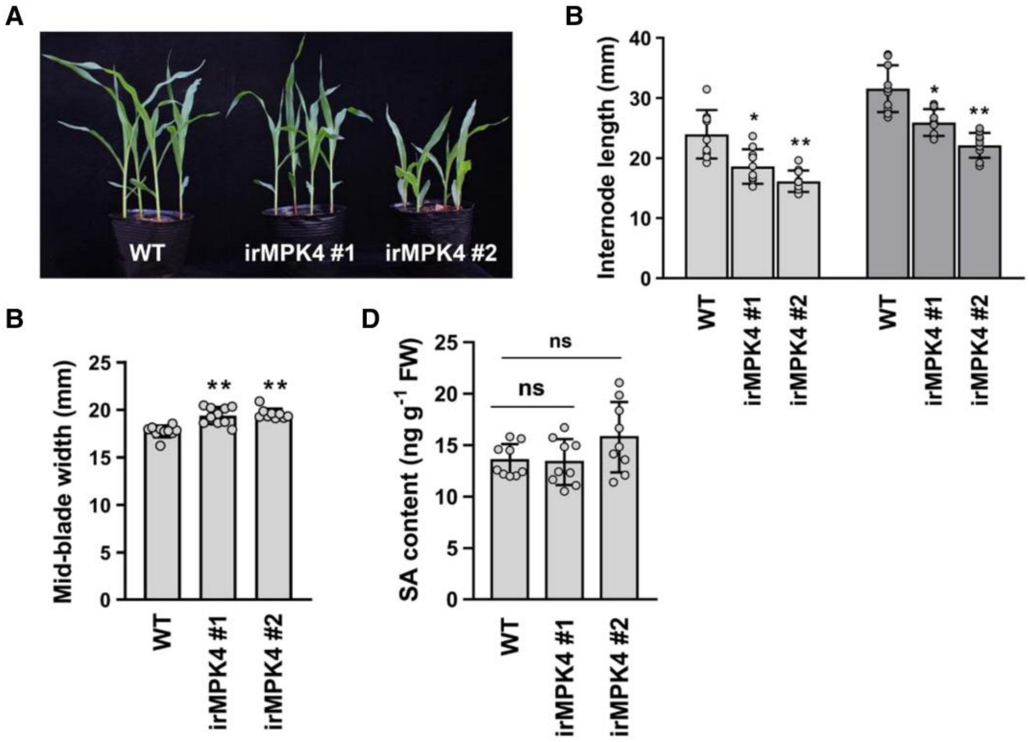

Figure 1. Growth and development-related traits of WT and irMPK4 transgenic lines. **A)** A photograph of 2-wk-old WT and irMPK4 transgenic plants (irMPK4 #1 and irMPK4 #2). **B)** Lengths of first (light gray bars) and second internodes (dark gray bars) measured from the base of the stem. **C)** Widths of third fully expanded leaves (mid-blade). **D)** SA levels in WT and irMPK4 transgenic plants under the basal condition. Data are means ± SD. Asterisks indicate significant differences between WT and irMPK4 line [Student's *t*-test; $^{*}P < 0.05$; $^{**}P < 0.01$; $n = 10$ for **B** and **C)**, and $n = 9$ for **D)**]. Similar results were obtained from at least 3 independent experiments, and representative images are shown.

(Supplementary Fig. S2). Under our greenhouse conditions, the irMPK4 transgenic lines had 20% to 30% shorter internodes compared with those of the WT plants (Fig. 1, A and B), whereas the blade widths of the third leaves of irMPK4 lines were about 10% bigger (Fig. 1C). Given that the Arabidopsis *mpk4* mutants accumulate high levels of SA and are severely dwarf (Petersen et al. 2000), we examined the SA accumulation in irMPK4 transgenic maize. Unlike the Arabidopsis *mpk4* mutants (1.3 μg/g; Petersen et al. 2000), the SA levels in the WT and irMPK4 lines were only between 10 and 20 ng/g (Fig. 1D), indicating that the reduced stature of MPK4 RNAi lines was not caused by the SA levels. Of note, these differences of internode lengths and leaf blade widths were no longer observed when these plants were mature and flowering.

Silencing *MPK4* compromises maize resistance to insects

First, whether *MPK4* is transcriptionally regulated in maize response to wounding and simulated herbivory was examined. Maize leaves were wounded with a pattern wheel, and 20 μL of water or oral secretions from the oriental armyworm (*M. separata*) were gently smeared on the wounds (WW and WOS treatments, respectively). After either treatment, *MPK4* transcripts were elevated about 10-fold at 0.5 h posttreatment and gradually declined, almost reaching the basal levels at 8 h (Supplementary Fig. S3).

Given the important role of JA in plant defense against herbivorous insects, we measured the JA and JA-Ile contents in the maize seedlings after the treatments of wounding and simulated *M. separata* insect herbivory. In the WT plants, JA and JA-Ile levels were strongly upregulated after both WW and WOS treatments at 1 h, and the JA and JA-Ile levels induced by WOS were higher than those induced by WW (Fig. 2A). Importantly, WW- and WOS-induced JA levels were respectively ∼85% and 75% higher in the irMPK4 transgenic lines than in the WT plants, and the WW- and WOS-induced JA-Ile levels were respectively ∼165% and 70% higher in the irMPK4 lines (Fig. 2A). At 2 h after WOS treatment, JA and JA-Ile levels in the irMPK4 lines were still higher than that in the WT plants, and 4 h after either treatment, JA-Ile but not JA levels remained elevated in the irMPK4 lines (Fig. 2A). Thus, MPK4 represses JA and JA-Ile biosynthesis induced by wounding or simulated insect herbivory.

Next, bioassays were performed for 10 d using the larvae of 3 lepidopteran insects, the oriental armyworm (*M. separata*), cotton leafworm (*S. litura*), and fall armyworm (*S. frugiperda*). The growth of 3 species of larvae on the irMPK4 transgenic lines was generally more rapid than on the WT plants (Fig. 2B): (i) *M. separata* larvae were heavier on both irMPK4 #1 and #2 than on the WT plants on all days examined. For example, on Day 10, the insects were 40% and 98% heavier on these 2 lines than on the WT plants; (ii) *S. litura* and *S. frugiperda* larvae were heavier on the irMPK4 #2 than on the WT plants on all days examined, respectively reaching 45% (Day 10) and 31% (Day 10) more than on the WT plants; however, on the irMPK4 #1, *S. litura* and *S. frugiperda* insects were heavier than on the WT plants only on Day 7 (13%) and Day 10 (11%), respectively. Thus, MPK4 is required for the resistance of maize to the specialist herbivore *M. separata*, and MPK4 also plays a minor role in maize resistance to the generalist herbivores *S. litura* and *S. frugiperda*. Similar results were obtained from another independent bioassay (Supplementary Fig. S4). After 10 d of *M. separata* feeding, the levels of DIM2BOA and HDM2BOA-Glc in both irMPK4 lines were lower than in the WT plants, and in line #2, HM2BOA-Glc levels were lower than in the WT plants (Supplementary Fig. S5);

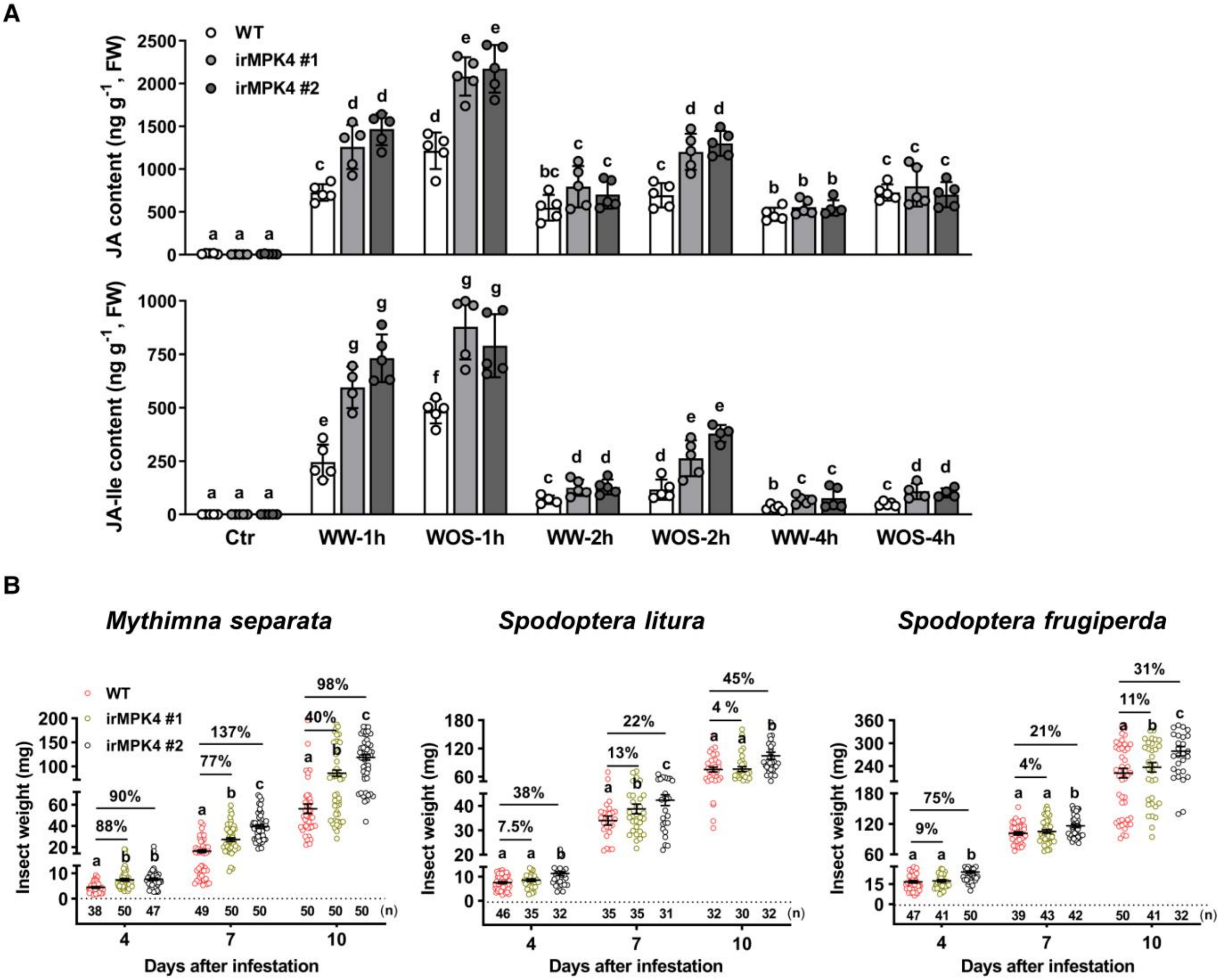

Figure 2. Silencing maize *MPK4* elevates wounding-induced or simulated herbivory-induced JA and JA-Ile levels but compromises maize resistance to lepidopteran insects. **A)** WW- and WOS-induced accumulation of JA and JA-Ile in WT and irMPK4 plants. WT and irMPK4 transgenic plants were treated with wounding (WW) or simulated *M. separata* herbivory (WOS), and samples were collected at 1, 2, and 4 h after treatments for quantification of JA and JA-Ile. Ctr, control, untreated plants. **B)** Larval growth of *M. separata*, *S. litura*, and *S. frugiperda* on WT and irMPK4 transgenic plants. Data are means ± SD. Different letters indicate significant differences [$P < 0.05$, 2-way ANOVA with post hoc Tukey's test, $n = 5$ for **A)**; $P < 0.05$, 1-way ANOVA with post hoc Tukey's test for **B)**, $n = 30$ to 50 and are indicated below each bar]. The percentages in **B)** stand for increases in the mean values of weight (mg) of the larvae reared on irMPK4 #1 or #2 compared with those on WT plants. Similar results were obtained from at least 3 independent experiments, and representative images are shown.

the levels of HDMBOA-Glc and DIM2BOA-Glc were greater in both irMPK4 transgenic lines, and DIMBOA, DIMBOA-Glc, and DIBOA-Glc had greater levels in irMPK4 line #2 than in WT plants (Supplementary Fig. S5). Thus, MPK4 is required for maize resistance to *M. separata*, and MPK4 regulates the levels of some Bxs in maize response to *M. separata* herbivory. Moreover, it is possible that certain unknown defensive metabolite(s), which is (are) positively regulated by MPK4, may also account for the increased insect growth phenotype of irMPK4 maize.

MPK4 is important for maize transcriptomic response to herbivory

Given the importance of transcriptional regulation in plant resistance to insects, we conducted an RNA-Seq analysis using 2-wk-old WT and irMPK4 #2 plants, which were elicited by WW and WOS and harvested after 1 and 8 h. In the WT plants, the expression of 5,730 and 6,020 genes was significantly changed, respectively, 1 h after WW and WOS treatment, compared with the untreated WT plants (Supplementary Table S1). These WW- and WOS-induced DEGs in the WT plants are termed as WW- and WOS-responsive DEGs, respectively. MPK4-regulated DEGs were also identified using pairwise comparison between the WT and irMPK4 plants with the same treatments at 1 h, and a total of 4,016 DEGs were found to be transcriptionally controlled by MPK4 (Fig. 3A; Supplementary Table S2). Venn diagram analysis indicated that among the DEGs induced by WW and WOS at 1 h, 26.3% (1,509 of 5,730) and 25.3% (1,522 of 6,020) were respectively regulated by MPK4 (Fig. 3A). We performed gene ontology (GO) analysis of biological processes on these 1,522 DEGs, which were both MPK4 regulated and WOS responsive. The resulted top 20 enriched terms included many biological processes related to protein posttranslational modification and hormone signaling pathways, which we grouped into the Group I and biological processes of stress-related responses (Group II), such as "response to stimulus" and "response to hydrogen peroxide" (Fig. 3B; Supplementary Fig. S6 and Table S3).

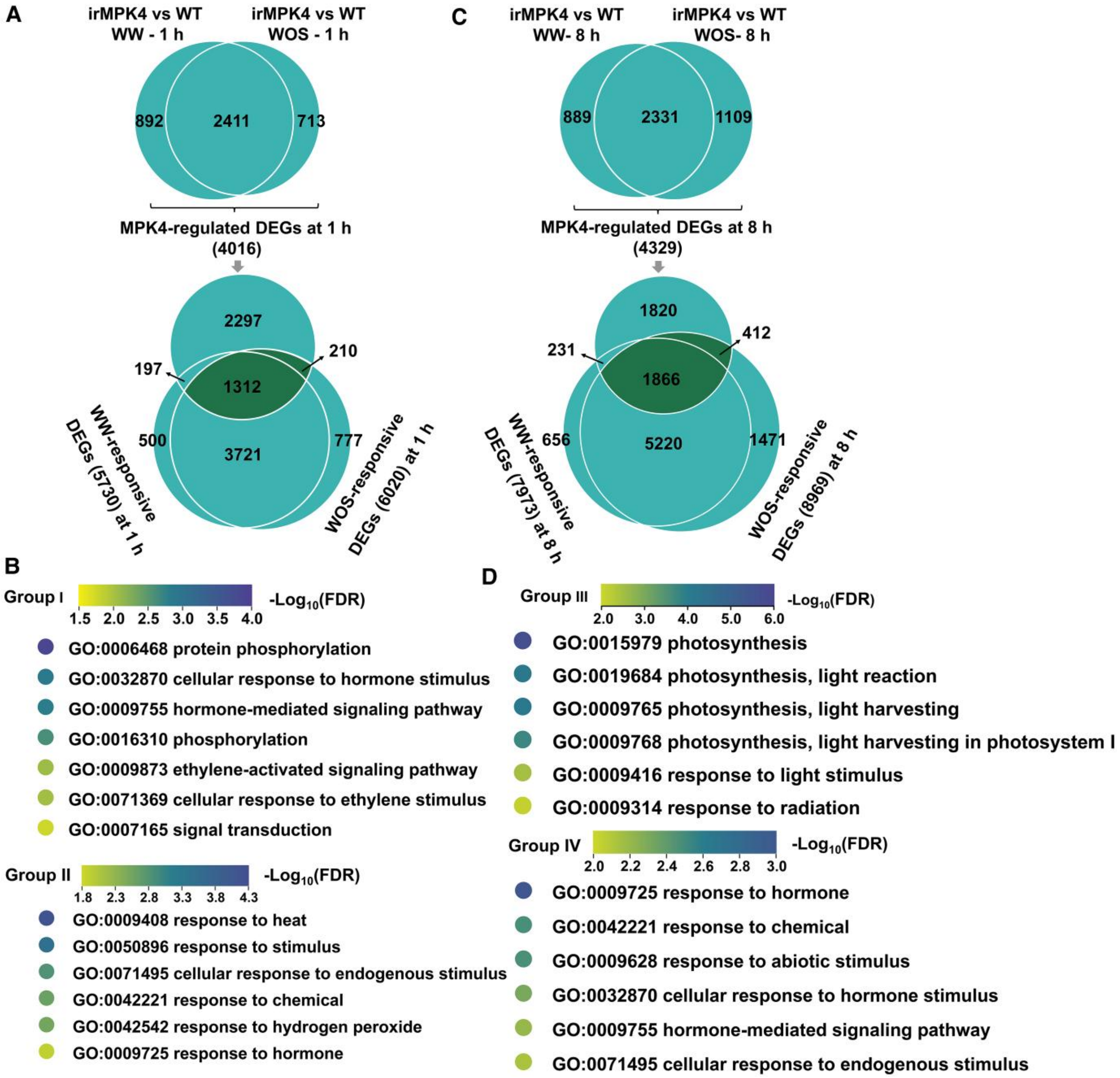

Figure 3. Comparisons of transcriptome responses of WT and irMPK4 plants with WW and WOS treatments. WT and irMPK4 #2 maize plants were treated with wounding (WW) or simulated *M. separata* herbivory (WOS). After 1 and 8 h, samples were harvested for RNA-seq analysis. **A)** Venn diagram analysis of the MPK4-regulated DEGs and WW- and WOS-responsive DEGs at 1 h. MPK4-regulated DEGs were identified by combining the DEGs obtained by comparing irMPK4 plants with WT plants. WW- and WOS-responsive DEGs were identified from the WW- and WOS-treated WT plants compared with the untreated WT plants. **B)** GO enrichment analysis of the 1,522 WOS-responsive and MPK4-regualted genes. These genes are highlighted with different color in **A)**. Two groups (I and II) of GO terms were selected from the top 20 enriched terms based on their relevance. **C)** Venn diagram analysis of the MPK4-regulated DEGs and WW- and WOS-responsive DEGs at 8 h. **D)** GO enrichment analysis of the 2,278 WOS-responsive and MPK4-regualted genes. These genes are highlighted with different color in **C)**. Two groups (III and IV) of GO terms were selected from the top 20 enriched terms based on their relevance.

Eight hours after elicitation by WW and WOS, 7,973 and 8,969 DEGs were respectively identified in the WT seedlings (Supplementary Table S4), and 4,329 genes were identified as MPK4-regulated DEGs (Fig. 3C; Supplementary Table S5). Venn diagram analysis indicated that 26.3% (2,097 of 7,973) and 24.6% (2,278 of 8,969) of WW-responsive and WOS-responsive DEGs were respectively controlled by MPK4 (Fig. 3C). The GO analysis of biological processes was also performed for the 2,278 DEGs, which were MPK4 regulated and WOS responsive. Among the top 20 terms, 6 were related to photosynthesis-related processes (Group III), and another 6 were related to hormone-related responses (Group IV; Fig. 3D; Supplementary Fig. S6 and Table S6).

Given the differences of *M. separata* feeding-elicited Bx contents between WT and irMPK4 plants, the transcript levels of genes in the Bx biosynthetic pathway were inspected. It was found that compared with that in the WT plants, the induced expression levels of most of *BX* genes except *BX7*, *BX8*, and *BX9* were reduced in the irMPK4 plants under either WW or WOS treatment (Supplementary Fig. S7, A and B). Moreover, consistent with our previous RT-qPCR result (Supplementary Fig. S1D), RNA-seq

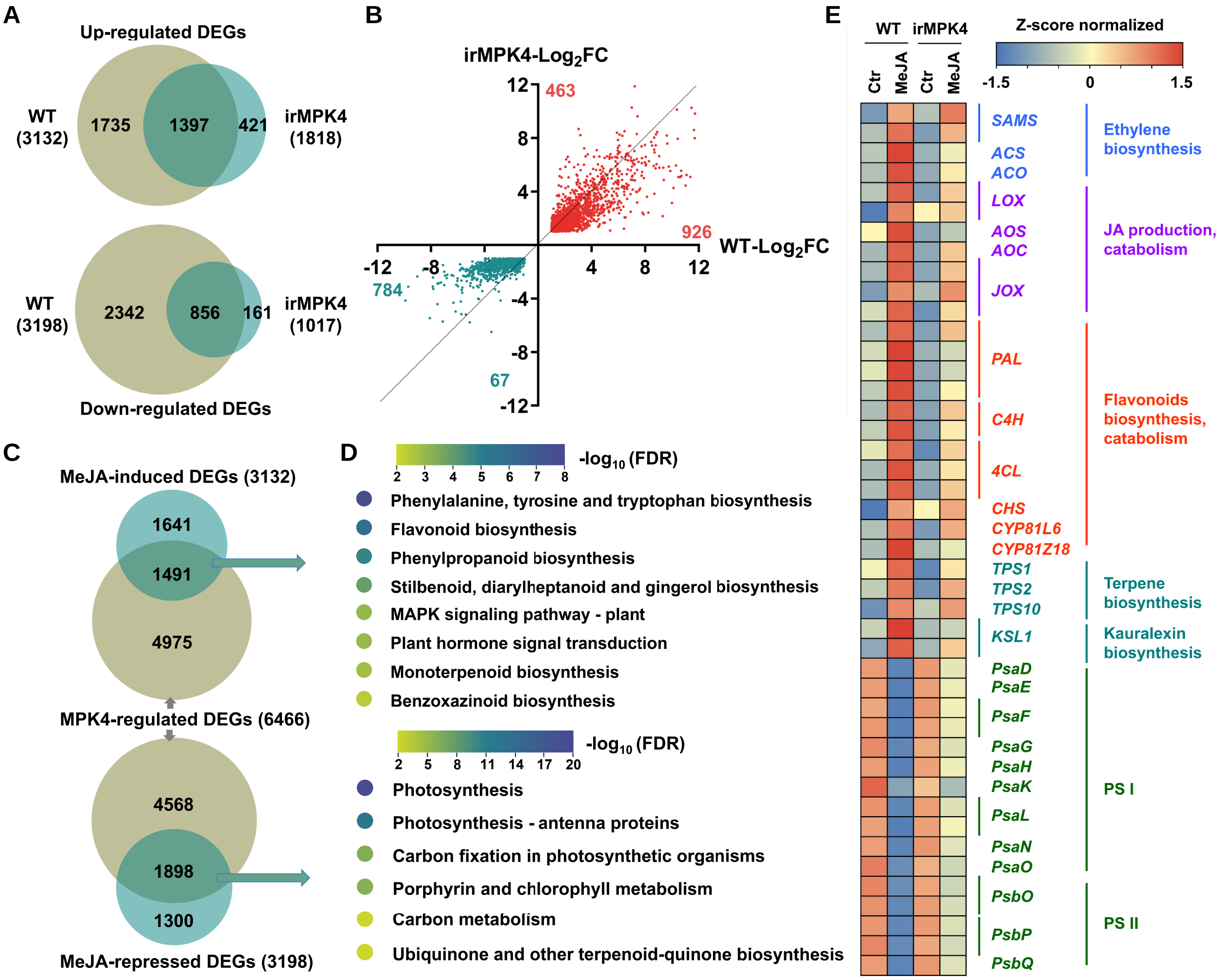

Figure 4. MPK4 is required for MeJA-induced genome-wide transcriptional changes. WT and irMPK4 #2 maize plants were treated with MeJA and harvested at 8 h for RNA-seq analysis. **A)** Venn diagram analysis of upregulated and downregulated DEGs in WT and irMPK4 plants in response to MeJA. **B)** Scatter plot indicating the fold changes of MeJA-responsive DEGs that were commonly regulated in WT and irMPK4 plants. Red and cyan dots represent upregulated and downregulated DEGs, respectively. $y = x$ line is shown. **C)** Venn diagram analysis of MeJA-induced or MeJA-repressed genes and MPK4-regulated genes. MeJA-induced or MeJA-repressed genes were identified between MeJA and control WT plants. MPK4-regulated DEGs were identified by comparing irMPK4 plants with WT plants under control and MeJA treatment. **D)** Representative terms from KEGG pathway enrichment analysis of 1,491 MeJA-induced MPK4-regulated genes (upper panel) and 1898 MeJA-repressed MPK4-regulated (lower panel) genes. **E)** Heatmap of DEGs of several pathways that had decreased induced in irMPK4 plants than in WT plants after MeJA treatment. Ctr, control (mock treatment).

data also confirmed the success of RNAi-mediated knockdown of *MPK4* in the irMPK4 #2 line, as shown in the RNA-seq genome browser screenshot (Supplementary Fig. S7C). These results suggest that MPK4 plays an important role in transcriptionally regulating WW- and WOS-responsive genes, including several Bx biosynthesis genes.

MPK4 regulates JA signaling

Our previous study suggested that the JA pathway plays a critical role in regulating herbivory-induced Bxs in maize (Ma et al. 2023). The irMPK4 plants had increased WOS-induced JA/JA-Ile accumulation (Fig. 2A) but exhibited decreased insect resistance (Fig. 2B). Thus, we speculated that MPK4 may be involved in the JA signaling.

To this end, the WT and irMPK4 #2 plants were treated with MeJA for 8 h and then harvested for RNA-Seq analysis (3 biological replicates for each sample group). By pairwise comparisons of MeJA-treated plants and control plants, we identified 6,330 DEGs (3,132 upregulated and 3,198 downregulated) in the WT plants, while only 2,835 DEGs (1,818 upregulated and 1,017 downregulated) were found in the irMPK4 plants (Fig. 4A; Supplementary Table S7), indicating decreased responsiveness to MeJA in the irMPK4 plants. Venn diagram analysis revealed that among the 3,132 upregulated and 3,198 downregulated DEGs in the WT plants, 55.4% (1,735 of 3,132) and 73.2% (2,342 of 3,198) of them were induced in the WT plants but not in the irMPK4 plants; these genes were no longer transcriptionally regulated by MeJA in the irMPK4 plants (Fig. 4A). Thus, MPK4 transcriptionally controls a large portion of MeJA-responsive genes. Venn diagram analysis also showed that 1,397 and 856 upregulated and downregulated DEGs were common between WT and irMPK4 plants (Fig. 4A). Next, a scatter plot indicating the fold-change values was used to visualize the regulation of these commonly regulated DEGs in the WT and irMPK4 plants. Among the 1,397 upregulated DEGs, 66.3% (926) were more strongly regulated in the WT plants than in the irMPK4 plants (Fig. 4B); more strikingly, 91.6% (784) of the downregulated DEGs (856 in total) exhibited greater downregulation in the WT plants than in the irMPK4 plants (Fig. 4B). Next, we sought to identify which MeJA-responsive genes are regulated by MPK4. First, these 3,132 upregulated and 3,198 downregulated genes that showed significant expression differences between the MeJA-treated and control WT plants were defined as the MeJA-responsive genes. Similarly, the 6,466 DEGs between the WT plants and irMPK4 plants under both control and MeJA treatment were defined as the MPK4-regulated genes (Supplementary Fig. S8A). Venn diagram analysis indicated that nearly half of MeJA-induced genes (47.6%, 1,491 of 3,132) and more than half of MeJA-repressed genes (59.3%, 1,898 of 3,198) were regulated by MPK4 (Fig. 4C; Supplementary Table S8), confirming that MPK4 plays an important role in the JA signaling pathway.

Kyoto Encyclopedia of Genes and Genomes (KEGG) pathway enrichment analysis revealed that the 1,491 MeJA-upregulated and MPK4-regulated genes were enriched in plant MAPK signaling pathway, plant hormone signal transduction, and biosynthesis of secondary metabolites, including flavonoid, phenylpropanoid, monoterpenoid, and benzoxazinoid (Fig. 4, D and E; Supplementary Tables S9 and S10). Moreover, KEGG analysis of the 1,898 MeJA-repressed and MPK4-regulated genes revealed enrichment in photosynthesis and photosynthesis-related biological processes (Fig. 4, D and E; Supplementary Tables S9 and S10). Moreover, Venn diagram analysis of the MPK4-regulated genes identified in this study and the MYC2-targeted genes identified by CUT&Tag analysis in our previous study (Ma et al. 2023) showed that more than half of MPK4-regulated genes are directly targeted by MYC2 (Supplementary Fig. S8B and Table S11). KEGG enrichment analysis revealed that the MPK4-regulated and MYC2-targeted genes were enriched in MAPK signaling pathway and biosynthesis of secondary metabolites (Supplementary Fig. S8B and Table S11), and the MPK4-regulated but not MYC2-targeted genes were mainly enriched in pathways related to photosynthesis (Supplementary Fig. S8B and Table S11). Collectively, these results indicate the indispensable role of MPK4 in modulating JA-induced transcriptional changes in maize.

Given the importance of Bxs in maize resistance to insects, the expression of *BX* genes was specifically quantified using RT-qPCR. Most of the *BX* genes were highly induced in the WT plants after MeJA treatment; however, *BX2*, *BX3*, *BX5*, *BX6*, *BX9*, *BX10*, *BX11*, *BX12*, *BX13*, and *BX14* were less induced in the irMPK4 plants (Supplementary Fig. S9), demonstrating the involvement of MPK4 in the MeJA-induced transcriptional regulation of these *BX* genes. On the level of defensive metabolites, we quantified the Bxs in the WT and irMPK4 plants after they were treated with MeJA for 48 h. In the WT plants, MeJA treatment markedly elevated the levels of several Bxs (HDMBOA-Glc, DIM2BOA-Glc, HM2BOA-Glc, and DIBOA-Glc), whereas the levels of DIMBOA-Glc, DIMBOA, and DIM2BOA were reduced (Supplementary Fig. S10). Notably, MeJA-induced HDMBOA-Glc, DIM2BOA-Glc, and HM2BOA-Glc in irMPK4 plants were much higher than in the WT plants, while HDM2BOA-Glc was lower in the irMPK4 plants (Supplementary Fig. S10).

MPK4 negatively regulates stability of MYC2s

Considering the central role of MYC2s in activating JA responses, maize MYC2s were chosen as the potential regulatory target of MPK4. First, whether the stability of 2 maize MYC2s, MYC2a and MYC2b, is controlled by MPK4 was examined. We performed a cell-free protein degradation assay by incubating the recombinant GST-MYC2a or GST-MYC2b protein with the total protein extracts from the WT and irMPK4 plants in the presence of ATP. Immunoblot analysis showed that GST-MYC2a was degraded after incubation with the total protein extract from the WT plants, whereas the degradation was much slower in the total protein extract from the irMPK4 plants (Fig. 5A). Adding MG132, an inhibitor of 26S proteasome activity, to the reaction largely blocked the degradation of GST-MYC2a (Fig. 5A), indicating that MPK4 affects MYC2a degradation by the 26S proteasome pathway. Similarly, the GST-MYC2b recombinant protein degraded much more rapidly in the total protein extracted from the WT plants than in the total protein extract from the irMPK4 transgenic plants, and the degradation was again partially blocked by the addition of MG132 (Fig. 5B). Notably, in the irMPK4 maize plants, degradation of GST-MYC2a and GST-MYC2b protein was only partially inhibited by MG132; thus, it is possible that in addition to MPK4, there are certain unknown regulators, which also control the stability of MYC2s, as shown in Arabidopsis that FERONIA phosphorylates and destabilizes MYC2 (Guo et al. 2018).

Next, to further confirm that maize MPK4 controls the stability of MYC2s, a construct expressing MYC2a-FLAG was cotransfected with the empty vector (EV, does not express any proteins) or with MPK4 or MPK4CA (D196G/E200A, a constitutively active version of MPK4; Berriri et al. 2012; Li et al. 2016). Indeed, overexpression of MPK4 clearly reduced the MYC2a-FLAG and MYC2b-FLAG protein levels, and coexpression of MPK4CA with MYC2a-FLAG or MYC2b-FLAG led to even further reduced MYC2a-FLAG or MYC2b-FLAG levels (Fig. 5C). Moreover, overexpressing MYC2a-FLAG in maize protoplasts isolated from the WT and irMPK4 plants resulted in higher protein levels of MYC2a-FLAG in the irMPK4 protoplasts than in the WT protoplasts (Fig. 5D). MYC2b-FLAG similarly exhibited a greater level in the irMPK4 protoplasts than in the WT protoplasts (Fig. 5D).

To study whether MPK4 regulates MYC2s' protein levels in planta, we generated a maize MYC2s-specific antibody using a synthetic peptide corresponding to the amino acid residues 501 to 515 of MYC2a or 493 to 507 of MYC2b. This antibody well recognized both MYC2a and MYC2b proteins expressed in maize protoplasts (Supplementary Fig. S11A) as well as WW-induced MYC2 proteins in the WT plants, but the corresponding band was absent in the *myc2ab* double mutants (Supplementary Fig. S11B), indicating that this antibody is maize MYC2s specific. The protein levels of MYC2s were induced 1 to 2 h after maize seedlings were treated with WW or WOS (Fig. 6A). As expected, the induced MYC2 protein levels in the irMPK4 plants were clearly higher than in the WT plants (Fig. 6A). Similar results were also obtained using the MeJA-treated WT and irMPK4 plants (Fig. 6B). To rule out the possibility that knockdown of *MPK4* affected *MYC2a* and *MYC2b* expression, we analyzed their relative transcript levels in all these plant samples used for immunoblotting. *MYC2a* and *MYC2b* expression levels were rapidly induced after WW, WOS, or MeJA treatment, but generally no significant differences were observed between the WT and irMPK4 plants (Supplementary Fig. S12).

MPK4 directly phosphorylates MYC2s for degradation

We next asked whether maize MPK4 interacts with and phosphorylates MYC2s. First, bimolecular fluorescence complementation (BiFC) and co-immunoprecipitation (Co-IP) were conducted, but these experiments did not indicate the interaction between MPK4 and MYC2a (Supplementary Fig. S13). To determine

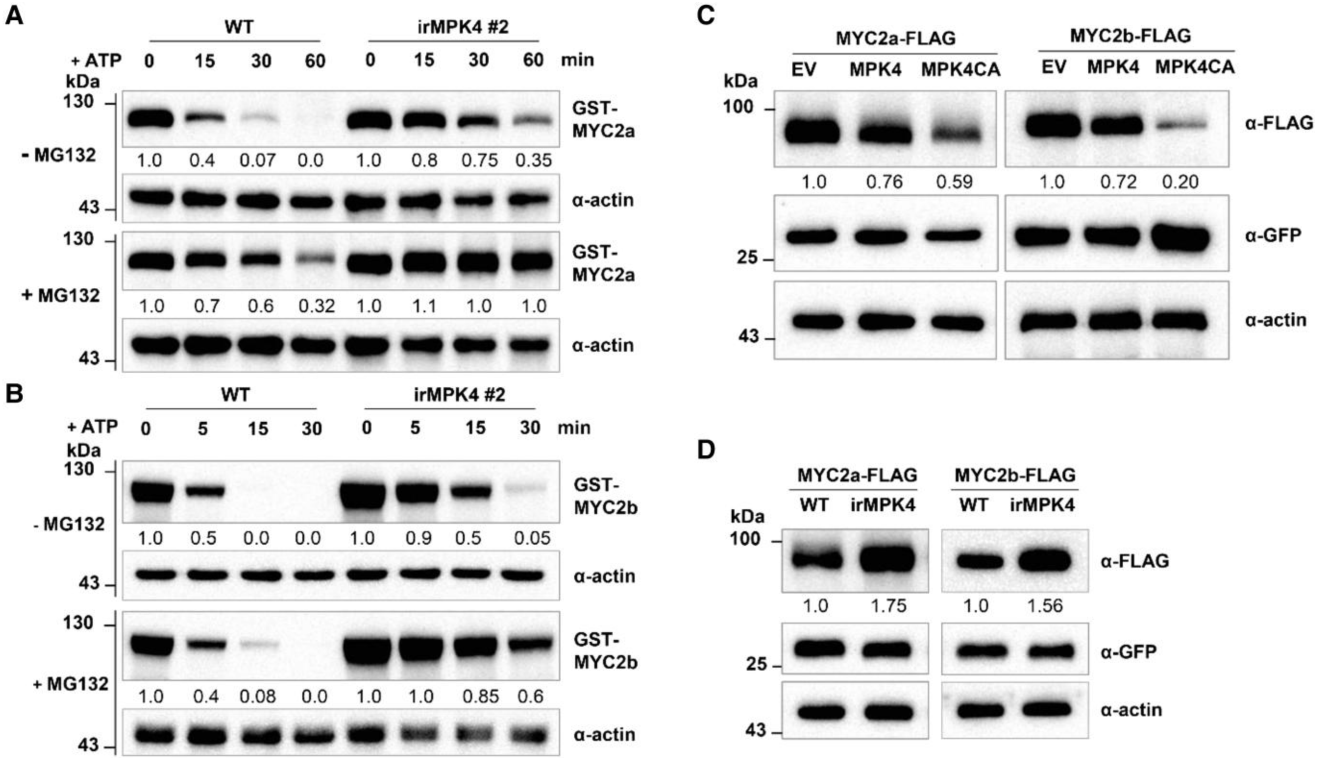

Figure 5. Maize MPK4 mediates degradation of MYC2a and MYC2b through 26S proteasome-dependent pathway. Levels of GST-MYC2a **A)** and GST-MYC2b **B)** in a cell-free degradation assay. Recombinant GST-MYC2a and GST-MYC2b proteins were incubated with equal amount of total protein extracted from WT and irMPK4 #2 plants in the presence of ATP with or without MG132. **C)** Coexpression analysis of MYC2a-FLAG with EV, MPK4, or MPK4CA in maize protoplasts. WT maize protoplasts were cotransfected with plasmids encoding MYC2a-FLAG and EV, MPK4, or MPK4CA (constitutively active version of MPK4). **D)** MYC2a-FLAG and MYC2b-FLAG levels in WT and irMPK4 protoplasts. Plasmids expressing MYC2a-FLAG or MYC2b-FLAG were transfected into maize protoplasts isolated from WT and irMPK4 #2 plants. For each protoplast transfection, the same amount of a plasmid harboring an *eGFP* gene was included, for assessing transfection efficiencies across samples. Anti-GST, anti-FLAG, anti-GFP, or antiactin was used for immunoblotting. Intensities of target protein bands were divided by band intensities of respective actin to obtain their relative intensities. The numbers shown in the images are values obtained by normalizing the relative intensities of target proteins with that of WT at 0 h **A** and **B)**, EV **C)**, or WT protoplasts **D)**, which were set as 1.0. Similar results were obtained from at least 3 independent experiments, and representative images are shown.

whether maize MYC2s can be phosphorylated in vivo, we performed phosphoprotein analysis using immunoprecipitated MYC2a-FLAG and MYC2b-FLAG from MeJA-treated WT protoplasts. MYC2a-FLAG and MYC2b-FLAG proteins were pulled down using anti-FLAG magnetic beads. Phosphoprotein analysis showed that the Thr115 and Thr112, 2 homologous sites in MYC2a-FLAG and MYC2b-FLAG, were phosphorylated (Fig. 7A; Supplementary Fig. S14, A and B) and consistent with the general feature of substrates of MAPKs (Bardwell 2006), and both the Thr phosphosites are followed by a proline (Supplementary Fig. S14, A and B). Next, we sought to determine whether maize MPK4 directly phosphorylates MYC2s. An in vitro phosphorylation assay was performed using recombinant His-MPK4CA and GST-MYC2a or GST-MYC2b followed by phosphoprotein analysis. Consistent with the findings of phosphosites of MYC2s in maize protoplasts, under the in vitro conditions, the identical Thr sites in GST-MYC2a and GST-MYC2b were phosphorylated by His-MPK4CA (Fig. 7A; Supplementary Fig. S14, C and D). His-GFP did not phosphorylate GST-MYC2a or GST-MYC2b. Thus, maize MPK4 directly phosphorylates MYC2a and MYC2b in vitro. It is likely that MPK4 only transiently interacts with MYC2s during phosphorylation, and subsequently MPK4 rapidly dissociates from MYC2a or MYC2b, making it very hard to detect their physical interactions using BiFC or Co-IP.

Specifically, the phosphosites of maize MYC2s were compared with the reported phosphosites of MYC2s from Arabidopsis (Zhai et al. 2013; Sethi et al. 2014; Guo et al. 2018; Zhu et al. 2023) and orange (Yue et al. 2023) and MYC2s from several monocots and eudicots, whose phosphosites are unknown (Supplementary Fig. S15). Sequence alignment indicated that these 2 homologous Thr sites in maize MYC2s are conserved in the monocots maize, *Sorghum bicolor*, *Oryza sativa*, *Brachypodium distachyon*, *Dendrobium catenatum*, and *Ananas comosus*, but not in the monocots *Asparagus officinalis* and *Yucca filamentosa* (Supplementary Fig. S15). Similarly, among the MYC2s in eudicots, the Ser123 of Arabidopsis MYC2, which is known to be a phosphosite and seems to be homologous to the Thr sites of maize MYC2s, was found to have homologous Ser sites of the MYC2s in *Solanum lycopersicum*, *Cucumis sativus*, and *Helianthus annuus*, but the MYC2s from *Citrus sinensis*, *Populus tremula* × *P. alba*, and *Glycine max* do not contain Ser at the homologous sites (Supplementary Fig. S15). Thus, the phosphosites of MYC2s are likely not conserved among plants.

Next, whether phosphorylation of Thr115 and Thr112 respectively affects MYC2a and MYC2b protein stability was analyzed. We mutated these Thr (T) sites of MYC2s to Ala (A), an amino acid that cannot be phosphorylated. MPK4 was coexpressed with 2 MYC2s or their mutants MYC2a^{T115A} and MYC2b^{T112A} in maize protoplasts. Unlike MYC2a and MYC2b, whose stability was strongly reduced by overexpression of MPK4, MYC2a^{T115A} and MYC2b^{T112A} protein levels were nearly not affected by MPK4 overexpression (Fig. 7B). These results indicate that in maize, MPK4 phosphorylates MYC2s, resulting in rapid degradation of the phosphorylated MYC2s.

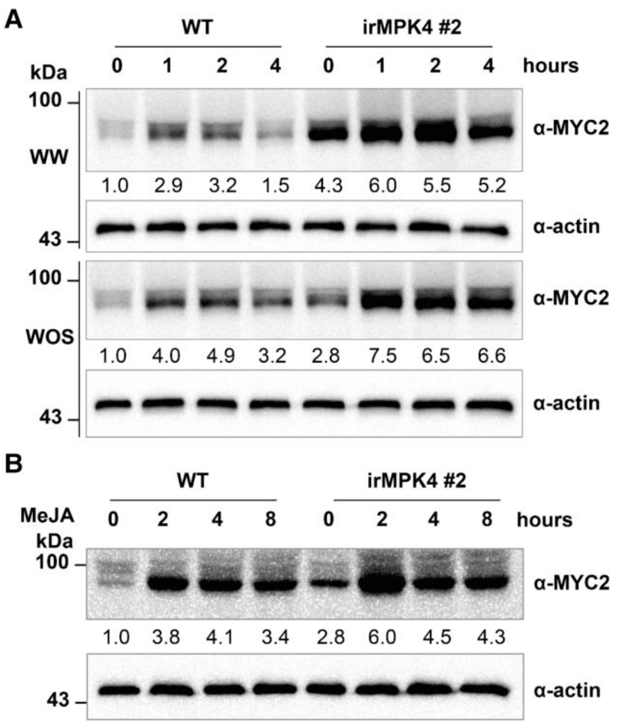

Figure 6. MPK4 negatively modulates levels of MYC2s in maize plants. Levels of MYC2s in WT and irMPK4 plants in response to WW or WOS **A)** or MeJA treatment **B)**. WT and irMPK4 plants were treated with WW, WOS, or 100 μM MeJA, and samples were harvested at the indicated times. MYC2s were detected with an anti-MYC2 antibody. Actin was used as the loading control. Note that the faint bands above the bands of MYC2s are nonspecific, which are not changed with time points. Relative intensity of each MYC2 band was obtained by dividing the intensity of MYC2 band by that of respective actin band. The numbers shown in the images are values obtained by normalizing the relative intensities of MYC2 bands with that of WT plants at 0 h, which was set as 1.0. Each sample was pooled from 4 biological replicates. Similar results were obtained from at least 3 independent experiments, and representative images are shown.

Transactivation activity of MYC2s on promoters of *BX* genes is regulated by phosphorylation and requires MPK4

Previous research has indicated that Arabidopsis MYC2 is modified by phosphorylation, and when the phosphosites of MYC2 were mutated to Ala, MYC2 protein exhibited decreased transactivation activity than did the WT MYC2 (Zhai et al. 2013; Zhu et al. 2023). Our recent study indicated that among the *BX* genes, *BX10/11/12/14* are highly inducible after MeJA treatment, and MYC2a and MYC2b directly bind to the promoters of these Bx biosynthesis genes to regulate their expression (Ma et al. 2023). Therefore, we compared the transactivation activity of MYC2a with MYC2a^{T115A} and MYC2b with MYC2b^{T112A} to the promoters of these 4 *BX* genes in the WT and irMPK4 protoplasts, using the dual luciferase assay. In the WT protoplasts, for the promoters of *BX10*, *BX11*, *BX12*, and *BX14*, MYC2a^{T115A}-FLAG showed 30% to 60% decreased activity than did MYC2a-FLAG (Fig. 8A), and compared with MYC2b-FLAG, MYC2b^{T112A}-FLAG showed 10% to 50% decreased activity (Fig. 8B). RT-qPCR analysis of the expression of *MYC2a-FLAG*, *MYC2a^{T115A}-FLAG*, *MYC2b-FLAG*, and *MYC2b^{T112A}-FLAG* ruled out the possibility of variation of transfection efficiencies within each experiment (Supplementary Fig. S16). These data suggest that phosphorylated MYC2s have greater transactivation activity than do the nonphosphorylated MYC2s.

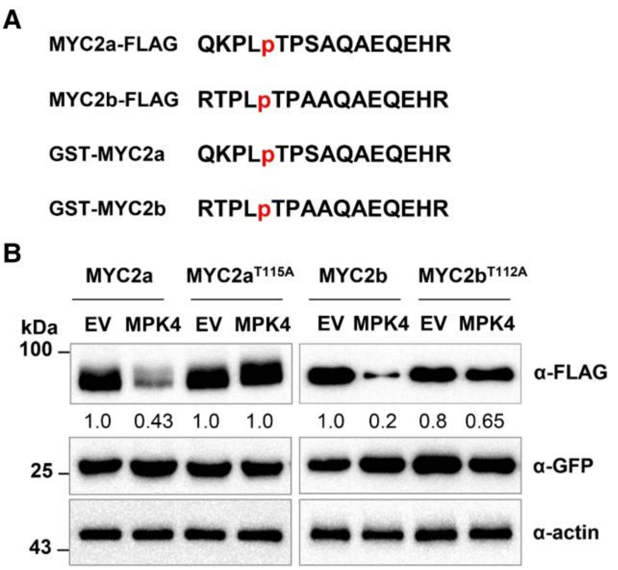

Figure 7. T115 in MYC2a and T112 in MYC2b are directly phosphorylated by MPK4, and the phosphorylated MYC2s are prone to degradation. **A)** Phosphosites of maize MYC2s (MYC2a: T115, MYC2b: T112) identified in vivo and in vitro. MYC2a-FLAG or MYC2b-FLAG proteins expressed in maize protoplasts were immunoprecipitated by anti-FLAG magnetic beads and subjected to phosphoprotein analysis. Recombinant GST-MYC2a or GST-MYC2b was incubated with constitutively active His-MPK4CA and then subjected to phosphoprotein analysis. The detected peptide sequences are shown. The p before each T represents phosphorylation. **B)** Effect of mutations of phosphosites on the stability of MYC2a-FLAG and MYC2b-FLAG. Plasmids expressing MYC2a-FLAG, MYC2a^{T115A}-FLAG, MYC2b-FLAG, or MYC2b^{T112A}-FLAG were respectively cotransfected with EV or a plasmid expressing MPK4 into WT maize protoplasts, and an anti-FLAG antibody was used to detect the FLAG-tagged proteins. For each protoplast transfection, the same amount of a plasmid harboring an *eGFP* gene was included, for assessing transfection efficiencies across samples. Intensities of target protein bands were divided by band intensities of respective actin to obtain their relative intensities. The numbers shown in the images are values obtained by normalizing the relative intensities of target proteins with those of EV, which were set as 1.0. Similar results were obtained from at least 3 independent experiments, and representative images are shown.

In the irMPK4 protoplasts, MYC2a-FLAG and MYC2b-FLAG exhibited 10% to 60% decreased transactivation activity levels than in the WT protoplasts (Fig. 8), supporting the previous finding from RNA-Seq analysis (Fig. 4, A and B) that MPK4 is required for the JA signaling. Furthermore, even though MYC2a^{T115A}-FLAG and MYC2b^{T112A}-FLAG cannot be phosphorylated, these 2 proteins still showed decreased transactivation activity in the irMPK4 protoplasts than in the WT protoplasts (Fig. 8), suggesting that MPK4 is required for the transactivation activity of MYC2s, regardless of whether MYC2s are phosphorylated or not. We hypothesize that MPK4 may phosphorylate and thus control the activity of an important factor that is required by both unphosphorylated and phosphorylated MYC2s for transactivation of downstream genes (Fig. 9).

Discussion

Many studies in eudicot species have shown that MAPKs are involved in plant growth and development and adaptation to stresses through phosphorylation of downstream targets (Zhang and Zhang 2022). However, little is known about the role of MAPKs in maize. This study reveals the requirement of MPK4 in the maize defensive response to insects, and importantly, we show that

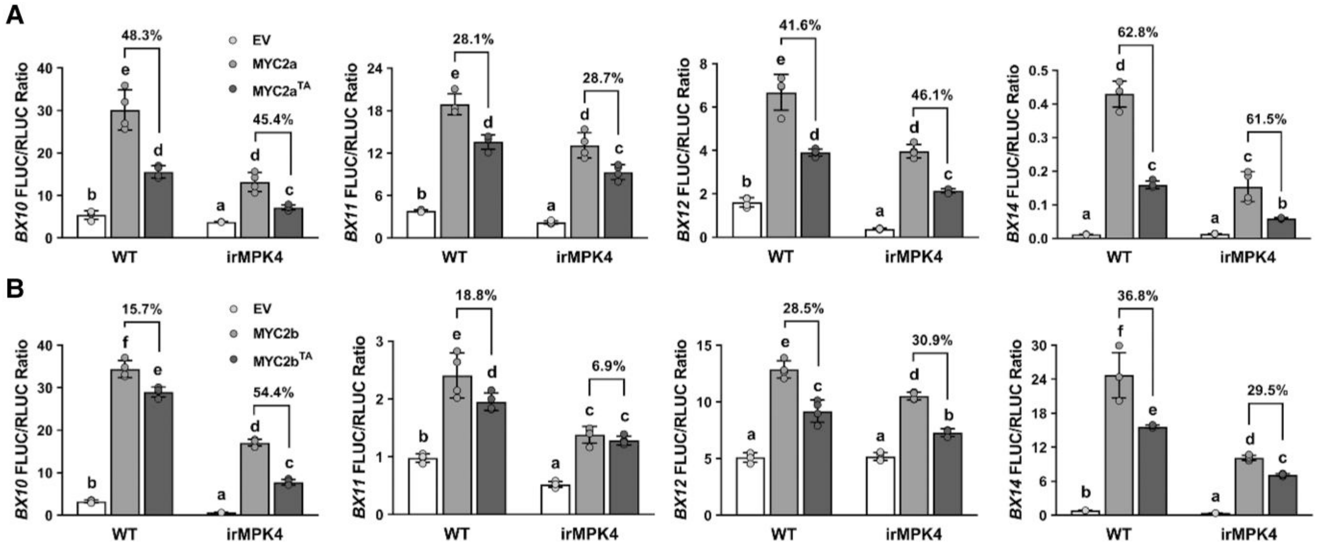

Figure 8. Thr115A mutation in MYC2a and Thr112A mutation in MYC2b reduce their transactivation activity to the promoters of *BX10*, *BX11*, *BX12*, and *BX14*. Transactivation activity of MYC2a-FLAG and MYC2a^{TA}-FLAG **A)** and MYC2b-FLAG and MYC2b^{TA}-FLAG **B)** to the promoters of *BX10*, *BX11*, *BX12*, and *BX14* was measured using a dual luciferase system in protoplasts from WT and irMPK4 line #2 maize protoplasts. EV plasmid was used for transfection as the control. Data are means ± SD. Different letters above the columns indicate significant differences (2-way ANOVA with Tukey's post hoc test; $P < 0.05$; $n = 4$). Similar results were obtained from at least 3 independent experiments, and representative data are shown.

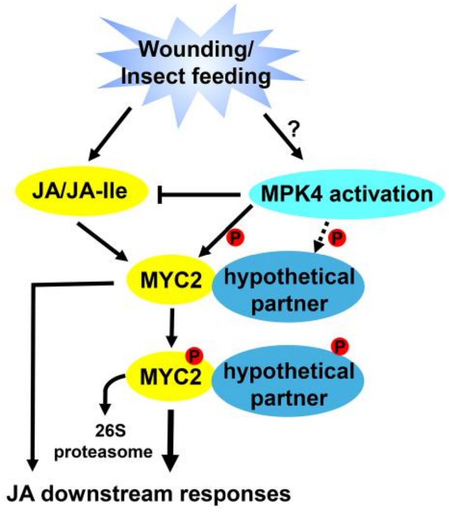

Figure 9. A working model for the role of MPK4 in maize defense against insects and JA signaling pathway. When maize is under insect attack, MPK4 may be rapidly activated. The levels of JA and JA-Ile rapidly increase and thus activating the JA signaling. MYC2s (MYC2a and MYC2b) are essential for maize JA signaling. Activated MPK4 directly phosphorylates MYC2s to enhance the transcriptional activity of MYC2s on downstream genes, and the phosphorylated MYC2s proteins are more prone to 26S proteasome-mediated degradation. MPK4 may also phosphorylate and thus regulate the activity of a hypothetical MYC2-interacting partner protein, which is required by both nonphosphorylated and phosphorylated MYC2s for their transcriptional activity. The letter P in a circle indicates phosphorylation process or phosphorylated form. Dashed arrow indicates a hypothetical pathway. Thickness of the arrows from MYC2 represents the relative transcriptional activity.

maize MPK4 has dual roles in JA signaling: (i) MPK4 directly phosphorylates MYC2s and thus destabilizes MYC2s and (ii) MPK4 is required by MYC2s for activation of various downstream responses.

In Arabidopsis, MYC2 protein is modified at the posttranslational level by phosphorylation and ubiquitination (Zhai et al. 2013; Jung et al. 2015; Guo et al. 2018; Chico et al. 2020; Zhu et al. 2023). The phosphorylation of MYC2 is probably often mediated by MAPKs. Sethi et al. (2014) found that blue light–activated MPK6 can phosphorylate MYC2 during Arabidopsis seedling development. Recently, Yue et al. (2023) reported that in orange (*C. sinensis*) jasmonate-induced MYC2 regulates *β*-citraurin biosynthesis and *MPK6* expression, which in turn phosphorylates MYC2 and promotes its turnover, therefore influencing fruit coloration. Using in vitro phosphorylation assay, we showed that maize MYC2s are directly phosphorylated by MPK4 (Fig. 7A; Supplementary Fig. S14, C and D). In maize, compared with the nonphosphorylatable forms, the phosphorylatable MYC2s in WT forms have higher transcriptional activity (Fig. 8), indicating that phosphorylated MYC2s have elevated transcriptional activity. This finding is similar to what was found in Arabidopsis: nonphosphorylatable Arabidopsis MYC2 showed decreased transcriptional activity than did the MYC2 in the WT form (Zhai et al. 2013; Zhu et al. 2023). Importantly, in maize, the phosphorylated MYC2s are prone to ubiquitination-mediated degradation and thus MPK4 regulates the stability of MYC2s (Fig. 7B). Similarly, in Arabidopsis, phosphorylated MYC2 is also subjected to degradation (Zhai et al. 2013; Guo et al. 2018). Comparison between the known phosphosites of MYC2s in maize (this study), Arabidopsis, and orange, and sequence alignment of MYC2s in a few monocots and eudicots suggested that the phosphosites of MYC2 are not conserved in different plant lineages (Supplementary Fig. S15). Thus, even though the functions of MYC2 in transducing JA signaling are very likely to be conserved, the posttranslational modifications of MYC2, which may regulate the activity and/or stability, evolved to be lineage specific. The evolution of posttranslational modifications of MYC2s is particularly interesting to study.

High JA/JA-Ile levels are usually associated with enhanced plant resistance to insects (Howe and Jander 2008). However, there seems a discrepancy between the increased JA/JA-Ile levels after WW and WOS treatment and the decreased insect resistance in the irMPK4 plants (Fig. 2, A and B). The reason for such a discrepancy is that maize MPK4 is also required by MYC2s to function in JA signaling (Fig. 9). Comparison of the transcriptomes of MeJA-treated WT and irMPK4 plants indicated that MPK4 is required for the transcriptional regulation of many JA-responsive genes: 55.4% and 73.2% of the upregulated and downregulated genes were completely MPK4 dependent (64% overall; Fig. 4A), and furthermore, even among the commonly regulated genes between WT and irMPK4 maize, many genes were more highly induced/repressed in the WT plants than in the irMPK4 plants (Fig. 4B). Our recent genetic study using maize *myc2ab* double mutants indicated that among 4,198 MeJA-responsive genes, 2,245 (53%) were dependent on MYC2s (Ma et al. 2023). It seems that maize MPK4 plays an even more important role in JA signaling than does MYC2s. Thus, even though after WW or WOS treatment, greater levels of JA and JA-Ile accumulated in the irMPK4 plants than in the WT plants, irMPK4 plants still exhibited decreased insect resistance, due to the severely compromised JA signaling.

It is noteworthy that MYC2s exhibited greater transcriptional activity to activate the genes of *BX10*/*BX11*/*BX12*/*BX14* in the WT protoplasts than in the irMPK4 protoplasts (Fig. 8), despite greater levels MYC2 protein were detected in the irMPK4 protoplasts than in the WT protoplasts. We hypothesize that MPK4 may also control the activity of certain partners of MYC2s by phosphorylation and finally influence the transcriptional activity of MYC2s (Fig. 9), e.g. the mediator subunit MED25 (Chen et al. 2012). Transactivation activity assay also suggested that this partner likely interacts with both phosphorylated and unphosphorylated MYC2s to enhance the activity of transcription (Fig. 9). The exact mechanism underlying how MPK4 is required by MYC2s to activate downstream transcriptional responses remains to be identified.

The expression of Bx biosynthesis genes is transcriptionally controlled by phytohormones and other signaling pathways and finally different transcription factors, including MYC2s. Nevertheless, on the metabolite level, the regulation of Bxs is very complex. The levels of individual Bxs are very dynamic, depending on the individual biosynthesis enzyme activity and contents/availability of indole (the precursor of all Bxs) and almost all the Bxs, which are under continuous conversion to the next Bxs on the pathway (Frey et al. 2009). MYC2s regulate the expression of all the 14 Bx biosynthesis genes: compared with those in the WT maize, after MeJA treatment, the transcript levels of all these Bx biosynthesis genes are much lower in the *myc2ab* mutants; however, among indole (precursor of all Bxs) and 16 Bxs, only 8 exhibited decreased levels in the *myc2ab* mutants, while the other 9 showed either no differences between *myc2ab* and WT maize or even greater levels in the *myc2ab* maize (Ma et al. 2023). Therefore, certain unknown mechanisms play important roles in the regulation of Bx metabolites. Among 14 Bx biosynthesis genes, MPK4 positively controls the expression of 11 genes (*BX1* to *BX6* and *BX10* to *BX14*) after WW or WOS treatment (Supplementary Fig. S7, A and B) and 10 genes (*BX2*, *BX3*, *BX5*, *BX6*, *BX9*, *BX10*, *BX11*, *BX12*, *BX13*, and *BX14*) after MeJA treatment (Supplementary Fig. S9). However, on the metabolite level, we did not find a good association correlation between MPK4 and Bxs (Supplementary Figs. S5 and S10). Thus, in addition to MYC2, MPK4 must also control other unknown factors, which are involved in the regulation of accumulation of Bxs. Given that bioassays indicated that silencing *MPK4* resulted in compromised resistance to insects, it is also likely that MPK4 also positively modulates the accumulation of one or more yet-to-be-identified defenses, in addition to Bxs.

MAPKs often regulate levels of phytohormones JA, SA, and ethylene (Jagodzik et al. 2018). Silencing *SIPK* or *WIPK* in *N. attenuata* led to reduced JA after wounding or simulated *M. sexta* feeding (Wu et al. 2007). Similarly, in tomato, silencing *LeMPK1* and *LeMPK2* also decreased wounding-induced JA levels (Kandoth et al. 2007). In irMPK4 maize plants, increased levels of JA were detected after WW or WOS treatments (Fig. 2A). Although MPK4 regulates SA levels in Arabidopsis and soybean (Petersen et al. 2000; Liu et al. 2011), MPK4 does not control SA levels in maize (Fig. 1D). Thus, it is unlikely that the increased WW- and WOS-induced JA levels were resulted from SA-JA antagonism (Thaler et al. 2012) in maize. Biosynthesis of JA is complex, as it is carried out serially in plastids and cytoplasm by many biosynthesis and catabolism enzymes and is controlled on both transcriptional and posttranscriptional levels (Wasternack and Hause 2013). Much research is still needed to understand how MPK4 regulate JA and JA-Ile levels.

Taken together, this study reveals at least dual roles of maize MPK4 in the JA signaling pathway and in response to insect herbivory. Maize MPK4 is a regulator that phosphorylates MYC2s and in turn controls MYC2s protein turnover, and MPK4 is also essential for MYC2 transcriptional activity (Fig. 9). Several questions remain to be answered: is there another protein that is regulated (e.g. phosphorylation) by MPK4 and this protein is required for MYC2s to activate the downstream transcriptional responses of MYC2s? Are there MYC2s-independent pathways in JA signaling that are also controlled by MPK4? Furthermore, in response to herbivory, how does maize regulate the activity of MPK4?

Materials and methods

Plant cultivation and treatments

Transformation of maize inbred line A188 (*Zea mays* L.) followed a previously published protocol (Ishida et al. 1996). WT and homozygous transgenic maize irMPK4 lines (irMPK4 #1 and #2) were grown in pots filled with Pindstrup substrate (www.pindstrup.com) and grown in the greenhouse with artificial light to supplement natural light (~12 to 14 h light, 10 to 12 h dark). The fully expanded third leaves of 2-wk-old maize seedlings (V3 stage) were used for all the experiments.

For mechanical wounding and simulated *M. separata* feeding, the third leaves of 2-wk-old maize seedlings were wounded with a pattern wheel to generate 2 rows of puncture wounds on each side of the midrib, and then immediately 20 μL of water or OS from *M. separata* larva was gently smeared on the wounds (named WW and WOS treatments, respectively). For measurement of internode lengths and leaf widths, 2-wk-old maize seedlings' first and second internode lengths and the third leaf widths were measured. For MeJA treatment, maize seedlings at the V3 stage were fully sprayed with 100 μM MeJA solution (containing 0.01% ethanol and 0.05% Tween 20) for 8 h, and plants treated with water containing 0.01% ethanol and 0.05% Tween 20 were used as the control.

Generation of constructs

The full-length coding sequences of *MPK4*, *MYC2a*, and *MYC2b* were amplified from the maize A188 cDNA. The partial sequence of MPK4 was cloned into the pHb7GW-I-WG-UBIL vector in an inverted-repeat fashion downstream of an ubiquitin promoter, forming the RNAi construct, which was used for transformation of maize. To obtain the EV plasmid, the *eGFP* coding region was removed from the vector pM999 by endonuclease digestion, and the resulted ends were ligated after a blunting treatment. Preparations of other constructs are described in the Supplementary data. Primers used for construct preparation are listed in the Supplementary Table S12.

Measurement of phytohormones and Bxs

Phytohormones JA, JA-Ile, and SA were measured as previously described (Song et al. 2022). Extraction and quantitation of Bxs followed a published method (Setotaw et al. 2024). The details are given in the Supplementary data.

RNA extraction, RT-qPCR, and RNA-Seq analysis

Detailed procedures for RNA sample preparation and RT-qPCR are described in the Supplementary data. For RNA-Seq analysis, 3 biological replicates were used, and each replicate was pooled from the third leaves collected from 3 individual plants of WT and irMPK4 #2 lines at the V3 stage. Each cDNA library was sequenced on an Illumina HiSeq 2500-PE125 platform at the sequencing depth of 5 Gb per sample. After trimming and filtering of poor-quality reads based on their quality scores, the resulting sequences were then aligned to maize A188 reference genome (Lin et al. 2021) using HISAT2 (Kim et al. 2015). Raw read counts per gene was obtained using FeatureCounts (Liao et al. 2014), and then DEGs were identified using the DESeq2 package (Love et al. 2014), based on the threshold that the false discovery rate (FDR) <0.01 and the absolute value of $\log_2$ (fold-change) >1. For GO analysis, PANTHER version 17 (http://pantherdb.org/) was used, and the FDR was set to 0.05. KEGG enrichment pathway analysis was performed using KOBAS (Xie et al. 2011) with the default parameters and the FDR was set to 0.05. Venn diagrams were generated using Biovenn (https://www.biovenn.nl/) (Hulsen et al. 2008). The TBtools toolkit (Chen et al. 2020) was used to generate heatmaps. RNA-Seq genome browser screenshot was generated using Integrative genomics viewer tool (Robinson et al. 2011).

Insect bioassay

Neonates of the oriental armyworm (*M. separata*), cotton leafworm (*S. litura*), and fall armyworm (*S. frugiperda*) were hatched from eggs (purchased from Henan Keyun Bio-Pesticides) in an incubator at 28 °C, and the neonates were reared on artificial diet for 3 to 4 d, and then these second-instar larvae were infested on plants. Approximately, 100 larvae were transferred to maize leaves of 2-wk-old seedlings of each genotype (32 plants, 3 to 4 larvae/plant). At the indicated days, mass of each larva was recorded.

Protein extraction and immunoblotting analysis

Proteins were extracted from pulverized leaf tissues or protoplasts using the extraction buffer (100 mM HEPES, pH 7.5, 5 mM EDTA, 5 mM EGTA, 10 mM NaF, 10 mM Na_3VO_4, 10 mM DTT, 50 mM β-glycerophosphate, 10% [v/v] glycerol) containing 1 protease inhibitor cocktail (Roche, Cat. #04693132001). Tissue debris were pelleted by centrifugation twice at 13,000 × *g* for 20 min at 4 °C. Protein concentrations were measured using the Bradford protein assay (Bio-Rad, Cat. #500-0205) with BSA as the standard, and protein samples were kept at −80 °C until use. For immunoblot analysis, 10 µg of total protein per lane were loaded. Actin was used to confirm equal protein loading. Immunoblot detection of proteins was performed using the following antibodies: anti-FLAG (Sigma-Aldrich, Cat: F7425), anti-GST (Beijing Protein Innovation, Cat. AbM59001-2H5-PU), anti-His_6 (Roche, Cat. 11922416001), anti-GFP (Santa Cruz, sc-9996), or antiactin (Abcam, Cat. ab197345). A custom-made anti-MYC2s antibody was used for detection of MYC2s of maize. The SuperSignal West Pico Plus Chemiluminescent Substrate (ThermoFisher, Cat. 34580) was used for the immunoblotting analysis. At least 3 replicates of western blot were performed, and besides the figures of western blot in the main text, the other 2 replicates of western blot were presented in Supplementary Fig. S17. For preparation of anti-MYC2s antibody, a synthetic peptide (amino acids 501 to 515) of MYC2a, which is identical to the amino acids 493 to 507 of MYC2b, was used as the antigen to immunize a New Zealand rabbit, and antigen-specific affinity chromatography was employed for purification of MYC2a/b antibody from the serum.

Maize protoplast transfection

Twelve-day-old maize etiolated seedlings were used for protoplast isolation and transfection, and the details can be found in the Supplementary data.

Phosphoprotein analysis of MYC2a and MYC2b in vivo

Maize protoplasts were transfected with plasmids expressing MYC2a-FLAG or MYC2b-FLAG. The protoplasts were treated with 50 µM MeJA for 2 h before being harvested. Protein extracted from the protoplasts was immunoprecipitated using anti-FLAG M2 magnetic beads (Sigma-Aldrich, Cat. M8823), and the purified MYC2a-FLAG and MYC2b-FLAG were confirmed by immunoblotting with the anti-FLAG antibody (Sigma-Aldrich, Cat. F7425). Identification of MYC2a and MYC2b phosphosites was done as described previously (Wu et al. 2019). In brief, the on-beads immunoprecipitated MYC2a-FLAG and MYC2b-FLAG and the freeze-dried in vitro phosphorylation reactions were suspended or reconstituted in trypsin digestion buffer and digested with trypsin at 37 °C for 16 h. The resulted peptides were used for phosphopeptide enrichment on TiO_2 beads. After being eluted from the TiO_2 beads, the enriched phosphopeptides were analyzed on a nano-flow LC-MS/MS (Orbitrap Exploris 480 [ThermoFisher]). The resulting raw data were processed with the MaxQuant software, and peptide spectra were searched against the maize A188 proteome database. The phosphorylation of serine, threonine, and tyrosine was included as variable modifications. Phosphosites were determined by the site-scanning algorithm search engine Andromeda. The FDR cutoffs were set to 0.01 for phosphosite assignment. The identified phosphorylated peptides were manually inspected to ensure confidence in phosphosite assignment. Mass spectrometry raw files can be found in the Supplementary data.

Preparation of recombinant proteins

Prokaryotic expression constructs were transformed into *Escherichia coli* strain BL21 (DE3; Sangon Biotech, Cat. #B528414). Recombinant protein expression was induced with 0.5 mM isopropylthio-β-galactoside at 22 °C. GST-tagged MYC2a and MYC2b (GST-MYC2a and GST-MYC2b) protein were purified using Proteinlso GST resin (TransGen Biotech, Cat. DP201), and His-tagged constitutively active MPK4 (His-MPK4CA) and GFP (His-GFP, as negative control) proteins were purified using Proteinlso Ni-NTA resin (TransGen Biotech, DP101). The purified recombinant proteins were used in in vitro phosphorylation assay and cell-free protein degradation assay in a cell-free system.

Cell-free protein degradation assay

Cell-free protein degradation assay was performed as previously described (Kong et al. 2015). In brief, total proteins were extracted from the third leaves of 2-wk-old WT and irMPK4 plants using native protein extraction buffer (50 mM Tris-MES, pH 8.0, 0.5 M sucrose, 10 mM EDTA, pH 8.0, 1 mM $MgCl_2$, 5 mM DTT) supplemented with 1 × cOmplete protease inhibitor cocktail (Roche). Protein concentrations were determined using Bradford method with BSA as the standard. Next, 100 μL of plant total protein extract (300 μg of total proteins) was incubated with 500 ng of purified recombinant proteins GST-MYC2a or GST-MYC2b with addition of 1 mM ATP. A final concentration of 50 μM MG132 was used for inhibition of 26S proteasome-mediated degradation of GST-MYC2a and GST-MYC2b proteins. After incubation at 25 °C, reaction aliquots were taken at the indicated time points, and were immediately stopped by addition of 4 × SDS loading buffer. Protein samples were subjected to immunoblotting and detected with an anti-GST antibody. Actin was used to evaluate the protein loading.

In vitro phosphorylation assay

The in vitro phosphorylation reaction was performed following a previously published method (Liu and Zhang 2004) with minor modifications. Recombinant GST-MYC2a or GST-MYC2b protein (3 μg) was mixed with 1 μg of the constitutively active His-MPK4CA or His-GFP (negative control) protein in the reaction buffer (20 mM Tris-HCl pH 7.5, 10 mM $MgCl_2$, 1 mM $MnCl_2$, 1 mM DTT, and 1 mM ATP). After incubation at 28 °C for 2 h, the reactions were freeze dried and used for LC-MS/MS analysis. Mass spectrometry raw files can be found in the Supplementary data.

Dual luciferase activity assay

The effector gene plasmids expressing MYC2a-FLAG or MYC2b-FLAG were cotransfected with the reporter gene plasmid (*ProBX10*:firefly-LUC, *ProBX11*:firely-LUC, *ProBX12*:firely-LUC, and *ProBX14*:firely-LUC) in maize protoplasts. After incubation in the dark at 25 °C for 16 h, the relative ratio of firefly-LUC: renilla-LUC was measured (TECAN, Infinite M200 PRO) to determine the transactivation activity relative to the control vector (i.e. protoplasts transfected with EV as effector and reporter gene plasmids), using the dual luciferase reporter assay system (Promega, Cat. E1910) according to the manufacturer's instructions.

BiFC and Co-IP

BiFC and Co-IP were conducted following previously published methods (Walter et al. 2004; Cheng et al. 2015). The details are given in the Supplementary data.

Accession numbers

Sequences from this study can be found in Maize Genetics and Genomics Database (MaizeGDB: https://www.maizegdb.org/) under the following accession numbers: *MPK4* (Zm00001d047349), *MPK3a* (Zm00001d047758), *MPK3b* (Zm00001d028711), *MPK6a* (Zm00001d036215), *MPK6b* (Zm00001d045310), *MYC2a* (Zm00001d030028), *MYC2b* (Zm00001d047017), and *eIF4A* (Zm00001d014673). The RNA-Seq data can be retrieved from the Beijing Institute of Genomics under the accession numbers PRJCA003190 and PRJCA003188.

Author contributions

J.W., J.L., and S.L. designed the study. J.L. and C.Z. created and screened the irMPK4 transgenic lines. S.L., J.L., C.M., M.Z., J.Q., and L.W. performed experiments or data analysis. S.L. and X.W. performed phosphosites identification. S.L., J.L., and J.W. wrote the manuscript.

Supplementary data

The following materials are available in the online version of this article.

Supplementary Figure S1. Phylogenetic analysis of MPK4 proteins, tissue-specific expression of *MPK4*, subcellular localization of MPK4 protein, and RNAi efficiency of irMPK4 transgenic lines.

Supplementary Figure S2. Expressions of *MPK3a*, *MPK3b*, *MPK6a*, and *MPK6b* genes are induced by WW and WOS treatment, but not affected by *MPK4* silencing.

Supplementary Figure S3. *MPK4* gene expression is induced by WW and WOS treatment.

Supplementary Figure S4. An independent bioassay supporting Fig. 2B.

Supplementary Figure S5. Relative abundance of Bxs in WT and irMPK4 maize after *Mythimna separata* feeding.

Supplementary Figure S6. Detailed description of GO enrichment analysis of Fig. 3, B and D.

Supplementary Figure S7. Heatmap analysis of relative expression levels of Bx biosynthetic genes and RNA-Seq genome browser screenshot of *MPK4* locus in WT and irMPK4 plants.

Supplementary Figure S8. KEGG enrichment analysis of MPK4-regulated and MYC2-targeted genes.

Supplementary Figure S9. Transcriptional profiles of all *BX* genes in WT and irMPK4 plants after MeJA treatment.

Supplementary Figure S10. MeJA-induced accumulation of Bxs in WT and irMPK4 plants.

Supplementary Figure S11. Confirmation of the specificity of custom-made antibody against maize MYC2s.

Supplementary Figure S12. Transcriptional regulation of *MYC2a* and *MYC2b* in WT and irMPK4 plants after WW, WOS, or MeJA treatment.

Supplementary Figure S13. BiFC and Co-IP analysis of interaction between MPK4 and MYC2s.

Supplementary Figure S14. Phosphosites of MYC2a at T115 and MYC2b at T112 identified in vivo and in vitro.

Supplementary Figure S15. Alignment of maize MYC2a and MYC2b with MYC2 proteins from species of monocots and eudicots.

Supplementary Figure S16. Relative expression levels of *MYC2a-FLAG* and *MYC2b-FLAG* in protoplasts isolated from WT and irMPK4 plants.

Supplementary Figure S17. Immunoblotting images of other replicates for Figs. 5, 6, and 7B.

Supplementary Table S1. WW- and WOS-induced DEGs in WT plants at 1 h.

Supplementary Table S2. MPK4-regulated DEGs at 1 h after WW and WOS treatment.

Supplementary Table S3. GO enrichment analysis of WOS-responsive and MPK4-regulated DEGs at 1 h.

Supplementary Table S4. WW- and WOS-induced DEGs in WT plants at 8 h.

Supplementary Table S5. MPK4-regulated DEGs at 8 h after WW and WOS treatment.

Supplementary Table S6. GO enrichment analysis of WOS-responsive and MPK4-regulated DEGs at 8 h.

Supplementary Table S7. MeJA-induced DEGs in WT plants.

Supplementary Table S8. MPK4-regulated DEGs with MeJA treatment.

Supplementary Table S9. KEGG pathway analysis of MeJA-responsive and MPK4-regulated DEGs.

Supplementary Table S10. DEGs of several pathways for heatmap.

Supplementary Table S11. KEGG pathway analysis of MPK4-regulated and MYC2-targeted genes.

Supplementary Table S12. List of primers used for RT-qPCR and construct preparation.

Funding

This study was supported by the National Natural Science Foundation of China (U23A20199 [J.W.], 32102301 [C.Z.], 32302464 [C.M.]), the Yunnan Revitalization Talent Support Program "Yunling Scholar" Project (J.W.), the Yunnan Innovation Team Project (202105AE160013 [J.W.]), the Strategic Priority Research Program of Chinese Academy of Sciences (XDPB16 [J.W.]), the General and Key Project of Applied Basic Research Program of Yunnan (202201AS070053 [J.Q.]), the CAS "Light of West China" Program (J.Q.), the China Postdoctoral Science Foundation (2019FD056 [S.L.], 2018M631111 [S.L.]), the Special Research Assistant of Chinese Academy of Sciences (C.M.), and the Postdoctoral Directional Training Foundation of Yunnan Province (S.L. and M.Z.).

Conflict of interest statement. None declared.

Data availability

The RNA-Seq data underlying this article can be retrieved from the Beijing Institute of Genomics (https://ngdc.cncb.ac.cn/gsub/) under the accession PRJCA003190 and PRJCA003188.

References

Andreasson E, Jenkins T, Brodersen P, Thorgrimsen S, Petersen NHT, Zhu S, Qiu J-L, Micheelsen P, Rocher A, Petersen M, *et al.* The MAP kinase substrate MKS1 is a regulator of plant defense responses. *EMBO J.* 2005:24(14):2579–2589. https://doi.org/10.1038/sj.emboj.7600737

Bardwell L. Mechanisms of MAPK signalling specificity. *Biochem Soc Trans.* 2006:34(5):837–841. https://doi.org/10.1042/BST0340837

Berriri S, Garcia AV, Frey N, Rozhon W, Pateyron S, Leonhardt N, Montillet J-L, Leung J, Hirt H, Colcombet J. Constitutively active mitogen-activated protein kinase versions reveal functions of Arabidopsis MPK4 in pathogen defense signaling. *Plant Cell.* 2012:24(10):4281–4293. https://doi.org/10.1105/tpc.112.101253

Betsiashvili M, Ahern KR, Jander G. Additive effects of two quantitative trait loci that confer (corn leaf aphid) resistance in maize inbred line Mo17. *J Exp Bot.* 2015:66(2):571–578. https://doi.org/10.1093/jxb/eru379

Chen C, Chen H, Zhang Y, Thomas HR, Frank MH, He Y, Xia R. TBtools: an integrative toolkit developed for interactive analyses of big biological data. *Mol Plant.* 2020:13(8):1194–1202. https://doi.org/10.1016/j.molp.2020.06.009

Chen R, Jiang H, Li L, Zhai Q, Qi L, Zhou W, Liu X, Li H, Zheng W, Sun J, *et al.* The Arabidopsis mediator subunit MED25 differentially regulates jasmonate and abscisic acid signaling through interacting with the MYC2 and ABI5 transcription factors. *Plant Cell.* 2012:24(7):2898–2916. https://doi.org/10.1105/tpc.112.098277

Cheng Z, Li J-F, Niu Y, Zhang X-C, Woody OZ, Xiong Y, Djonovic S, Millet Y, Bush J, McConkey BJ, *et al.* Pathogen-secreted proteases activate a novel plant immune pathway. *Nature.* 2015:521(7551):213–216. https://doi.org/10.1038/nature14243

Chico JM, Lechner E, Fernandez-Barbero G, Canibano E, Garcia-Casado G, Franco-Zorrilla JM, Hammann P, Zamarreno AM, Garcia-Mina JM, Rubioa V, *et al.* CUL3(BPM) E3 ubiquitin ligases regulate MYC2, MYC3, and MYC4 stability and JA responses. *Proc Natl Acad Sci U S A.* 2020:117(11):6205–6215. https://doi.org/10.1073/pnas.1912199117

Chini A, Fonseca S, Fernández G, Adie B, Chico JM, Lorenzo O, García-Casado G, López-Vidriero I, Lozano FM, Ponce MR, *et al.* The JAZ family of repressors is the missing link in jasmonate signalling. *Nature.* 2007:448(7154):666–671. https://doi.org/10.1038/nature06006

Christensen SA, Nemchenko A, Borrego E, Murray I, Sobhy IS, Bosak L, DeBlasio S, Erb M, Robert CAM, Vaughn KA, *et al.* The maize lipoxygenase, *ZmLOX10*, mediates green leaf volatile, jasmonate and herbivore-induced plant volatile production for defense against insect attack. *Plant J.* 2013:74(1):59–73. https://doi.org/10.1111/tpj.12101

De Geyter N, Gholami A, Goormachtig S, Goossens A. Transcriptional machineries in jasmonate-elicited plant secondary metabolism. *Trends Plant Sci.* 2012:17(6):349–359. https://doi.org/10.1016/j.tplants.2012.03.001

Deutsch CA, Tewksbury JJ, Tigchelaar M, Battisti DS, Merrill SC, Huey RB, Naylor RL. Increase in crop losses to insect pests in a warming climate. *Science.* 2018:361(6405):916–919. https://doi.org/10.1126/science.aat3466

Divekar PA, Narayana S, Divekar BA, Kumar R, Gadratagi BG, Ray A, Singh AK, Rani V, Singh V, Singh AK, *et al.* Plant secondary metabolites as defense tools against herbivores for sustainable crop protection. *Int J Mol Sci.* 2022:23(5):2690. https://doi.org/10.3390/ijms23052690

Erb M, Reymond P. Molecular interactions between plants and insect herbivores. *Annu Rev Plant Biol.* 2019:70(1):527–557. https://doi.org/10.1146/annurev-arplant-050718-095910

Fonseca S, Chini A, Hamberg M, Adie B, Porzel A, Kramell R, Miersch O, Wasternack C, Solano R. (+)-7-iso-Jasmonoyl-L-isoleucine is the endogenous bioactive jasmonate. *Nat Chem Biol.* 2009:5(5):344–350. https://doi.org/10.1038/nchembio.161

Frey M, Schullehner K, Dick R, Fiesselmann A, Gierl A. Benzoxazinoid biosynthesis, a model for evolution of secondary metabolic pathways in plants. *Phytochem.* 2009:70(15–16):1645–1651. https://doi.org/10.1016/j.phytochem.2009.05.012

Gu L, Liu Y, Zong X, Liu L, Li DP, Li DQ. Overexpression of maize mitogen-activated protein kinase gene, *ZmSIMK1* in Arabidopsis increases tolerance to salt stress. *Mol Biol Rep.* 2010:37(8):4067–4073. https://doi.org/10.1007/s11033-010-0066-6

Guo H, Nolan TM, Song G, Liu S, Xie Z, Chen J, Schnable PS, Walley JW, Yin Y. FERONIA receptor kinase contributes to plant immunity by suppressing jasmonic acid signaling in *Arabidopsis thaliana*. *Curr Biol.* 2018:28(20):3316–3324. https://doi.org/10.1016/j.cub.2018.07.078

Handrick V, Robert CAM, Ahern KR, Zhou S, Machado RAR, Maag D, Glauser G, Fernandez-Penny FE, Chandran JN, Rodgers-Melnik E, *et al.* Biosynthesis of 8-O-methylated benzoxazinoid defense compounds in maize. *Plant Cell.* 2016:28(7):1682–1700. https://doi.org/10.1105/tpc.16.00065

Hettenhausen C, Baldwin IT, Wu J. Silencing *MPK4* in *Nicotiana attenuata* enhances photosynthesis and seed production but compromises abscisic acid-induced stomatal closure and guard cell-mediated resistance to *Pseudomonas syringae* pv tomato DC3000. *Plant Physiol.* 2012:158(2):759–776. https://doi.org/10.1104/pp.111.190074

Hettenhausen C, Baldwin IT, Wu J. *Nicotiana attenuata* MPK4 suppresses a novel jasmonic acid (JA) signaling-independent defense pathway against the specialist insect *Manduca sexta*, but is not required for the resistance to the generalist *Spodoptera littoralis*. *New Phytol*. 2013:199(3):787–799. https://doi.org/10.1111/nph.12312

Howe GA, Jander G. Plant immunity to insect herbivores. *Annu Rev Plant Biol*. 2008:59(1):41–66. https://doi.org/10.1146/annurev.arplant.59.032607.092825

Hulsen T, de Vlieg J, Alkema W. BioVenn - a web application for the comparison and visualization of biological lists using area-proportional Venn diagrams. *BMC Genomics*. 2008:9(1):488. https://doi.org/10.1186/1471-2164-9-488

Ishida Y, Saito H, Ohta S, Hiei Y, Komari T, Kumashiro T. High efficiency transformation of maize (*Zea mays* L) mediated by *Agrobacterium tumefaciens*. *Nat Biotechnol*. 1996:14(6):745–750. https://doi.org/10.1038/nbt0696-745

Jagodzik P, Tajdel-Zielinska M, Ciesla A, Marczak M, Ludwikow A. Mitogen-activated protein kinase cascades in plant hormone signaling. *Front Plant Sci*. 2018:9:1387. https://doi.org/10.3389/fpls.2018.01387

Jeong JS, Jung C, Seo JS, Kim JK, Chua NH. The deubiquitinating enzymes UBP12 and UBP13 positively regulate MYC2 levels in jasmonate responses. *Plant Cell*. 2017:29(6):1406–1424. https://doi.org/10.1105/tpc.17.00216

Jung C, Zhao P, Seo JS, Mitsuda N, Deng S, Chua NH. PLANT U-BOX PROTEIN10 regulates MYC2 stability in Arabidopsis. *Plant Cell*. 2015:27(7):2016–2031. https://doi.org/10.1105/tpc.15.00385

Kandoth PK, Ranf S, Pancholi SS, Jayanty S, Walla MD, Miller W, Howe GA, Lincoln DE, Stratmann JW. Tomato MAPKs LeMPK1, LeMPK2, and LeMPK3 function in the systemin-mediated defense response against herbivorous insects. *Proc Natl Acad Sci U S A*. 2007:104(29):12205–12210. https://doi.org/10.1073/pnas.0700344104

Kazan K, Manners JM. MYC2: the master in action. *Mol Plant*. 2013:6(3):686–703. https://doi.org/10.1093/mp/sss128

Kim D, Landmead B, Salzberg SL. HISAT: a fast spliced aligner with low memory requirements. *Nat Methods*. 2015:12(4):357–360. https://doi.org/10.1038/nmeth.3317

Kong L, Cheng J, Zhu Y, Ding Y, Meng J, Chen Z, Xie Q, Guo Y, Li JG, Yang S, *et al*. Degradation of the ABA co-receptor ABI1 by PUB12/13 U-box E3 ligases. *Nat Commun*. 2015:6(1):8630. https://doi.org/10.1038/ncomms9630

Li S, Wang W, Gao J, Yin K, Wang R, Wang C, Petersen M, Mundy J, Qiu JL. MYB75 phosphorylation by MPK4 is required for light-induced anthocyanin accumulation in Arabidopsis. *Plant Cell*. 2016:28(11):2866–2883. https://doi.org/10.1105/tpc.16.00130

Liao Y, Smyth GK, Shi W. featureCounts: an efficient general purpose program for assigning sequence reads to genomic features. *Bioinformatics*. 2014:30(7):923–930. https://doi.org/10.1093/bioinformatics/btt656

Lin G, He C, Zheng J, Koo DH, Le H, Zheng H, Tamang TM, Lin J, Liu Y, Zhao M, *et al*. Chromosome-level genome assembly of a regenerable maize inbred line A188. *Genome Biol*. 2021:22(1):175. https://doi.org/10.1186/s13059-021-02396-x

Liu JZ, Horstman HD, Braun E, Graham MA, Zhang C, Navarre D, Qiu WL, Lee Y, Nettleton D, Hill JH, *et al*. Soybean homologs of MPK4 negatively regulate defense responses and positively regulate growth and development. *Plant Physiol*. 2011:157(3):1363–1378. https://doi.org/10.1104/pp.111.185686

Liu Y, Zhang D, Wang L, Li D. Genome-wide analysis of mitogen-activated protein kinase gene family in maize. *Plant Mol Biol Rep*. 2013:31(6):1446–1460. https://doi.org/10.1007/s11105-013-0623-y

Liu Y, Zhang S. Phosphorylation of 1-aminocyclopropane-1-carboxylic acid synthase by MPK6, a stress-responsive mitogen-activated protein kinase, induces ethylene biosynthesis in Arabidopsis. *Plant Cell*. 2004:16(12):3386–3399. https://doi.org/10.1105/tpc.104.026609

Love MI, Huber W, Anders S. Moderated estimation of fold change and dispersion for RNA-seq data with DESeq2. *Genome Biol*. 2014:15(12):550. https://doi.org/10.1186/s13059-014-0550-8

Ma C, Li R, Sun Y, Zhang M, Li S, Xu Y, Song J, Li J, Qi J, Wang L, *et al*. ZmMYC2s play important roles in maize responses to simulated herbivory and jasmonate. *J Integr Plant Biol*. 2023:65(4):1041–1058. https://doi.org/10.1111/jipb.13404

Meihls LN, Handrick V, Glauser G, Barbier H, Kaur H, Haribal MM, Lipka AE, Gershenzon J, Buckler ES, Erb M, *et al*. Natural variation in maize aphid resistance is associated with 2,4-dihydroxy-7-methoxy-1,4-benzoxazin-3-one glucoside methyltransferase activity. *Plant Cell*. 2013:25(6):2341–2355. https://doi.org/10.1105/tpc.113.112409

Meng X, Zhang S. MAPK cascades in plant disease resistance signaling. *Annu Rev Phytopathol*. 2013:51(1):245–266. https://doi.org/10.1146/annurev-phyto-082712-102314

Niemeyer H. Hydroxamic acids derived from 2-hydroxy-2H-1,4-benzoxazin-3(4H)-one: key defense chemicals of cereals. *J Agric Food Chem*. 2009:57(5):1677–1696. https://doi.org/10.1021/jf8034034

Petersen M, Brodersen P, Naested H, Andreasson E, Lindhart U, Johansen B, Nielsen HB, Lacy M, Austin MJ, Parker JE, *et al*. Arabidopsis MAP kinase 4 negatively regulates systemic acquired resistance. *Cell*. 2000:103(7):1111–1120. https://doi.org/10.1016/S0092-8674(00)00213-0

Qi J, Sun G, Wang L, Zhao C, Hettenhausen C, Schuman MC, Baldwin IT, Li J, Song J, Liu Z, *et al*. Oral secretions from *Mythimna separata* insects specifically induce defence responses in maize as revealed by high-dimensional biological data. *Plant Cell Environ*. 2016:39(8):1749–1766. https://doi.org/10.1111/pce.12735

Richter A, Powell AF, Mirzaei M, Wang LJ, Movahed N, Miller JK, Piñeros MA, Jander G. Indole-3-glycerolphosphate synthase, a branchpoint for the biosynthesis of tryptophan, indole, and benzoxazinoids in maize. *Plant J*. 2021:106(1):245–257. https://doi.org/10.1111/tpj.15163

Robinson JT, Thorvaldsdóttir H, Winckler W, Guttman M, Lander ES, Getz G, Mesirov JP. Integrative genomics viewer. *Nat Biotechnol*. 2011:29(1):24–26. https://doi.org/10.1038/nbt.1754

Rodriguez M, Petersen M, Mundy J. Mitogen-activated protein kinase signaling in plants. *Annu Rev Plant Biol*. 2010:61(1):621–649. https://doi.org/10.1146/annurev-arplant-042809-112252

Savary S, Willocquet L, Pethybridge SJ, Esker P, McRoberts N, Nelson A. The global burden of pathogens and pests on major food crops. *Nat Ecol Evol*. 2019:3(3):430–439. https://doi.org/10.1038/s41559-018-0793-y

Sethi V, Raghuram B, Sinha AK, Chattopadhyay S. A mitogen-activated protein kinase cascade module, MKK3-MPK6 and MYC2, is involved in blue light-mediated seedling development in Arabidopsis. *Plant Cell*. 2014:26(8):3343–3357. https://doi.org/10.1105/tpc.114.128702

Setotaw YB, Li J, Qi J, Ma C, Zhang M, Huang C, Wang L, Wu J. Salicylic acid positively regulates maize defenses against lepidopteran insects. *Plant Divers*. 2024:46(4):519–529. https://doi.org/10.1016/j.pld.2024.03.004

Sheard LB, Tan X, Mao H, Withers J, Ben-Nissan G, Hinds TR, Kobayashi Y, Hsu FF, Sharon M, Browse J, *et al*. Jasmonate perception by inositol-phosphate-potentiated COI1-JAZ co-receptor. *Nature*. 2010:468(7322):400–405. https://doi.org/10.1038/nature09430

Song J, Bian J, Xue N, Xu Y, Wu J. Inter-species mRNA transfer among green peach aphids, dodder parasites, and cucumber host plants. *Plant Divers*. 2022:44(1):1–10. https://doi.org/10.1016/j.pld.2021.03.004

Srivastava M, Srivastava AK, Roy D, Mansi M, Gough C, Bhagat PK, Zhang CJ, Sadanandom A. The conjugation of SUMO to the transcription factor MYC2 functions in blue light-mediated seedling development in Arabidopsis. *Plant Cell*. 2022:34(8):2892–2906. https://doi.org/10.1093/plcell/koac142

Staswick PE, Tiryaki I. The oxylipin signal jasmonic acid is activated by an enzyme that conjugates it to isoleucine in Arabidopsis. *Plant Cell*. 2004:16(8):2117–2127. https://doi.org/10.1105/tpc.104.023549

Thaler JS, Humphrey PT, Whiteman NK. Evolution of jasmonate and salicylate signal crosstalk. *Trends Plant Sci*. 2012:17(5):260–270. https://doi.org/10.1016/j.tplants.2012.02.010

Thines B, Katsir L, Melotto M, Niu Y, Mandaokar A, Liu G, Nomura K, He SY, Howe GA, Browse J. JAZ repressor proteins are targets of the SCF complex during jasmonate signalling. *Nature*. 2007:448(7154):661–665. https://doi.org/10.1038/nature05960

Tzin V, Fernandez-Pozo N, Richter A, Schmelz EA, Schoettner M, Schäfer M, Ahern KR, Meihls LN, Kaur H, Huffaker A, *et al*. Dynamic maize responses to aphid feeding are revealed by a time series of transcriptomic and metabolomic assays. *Plant Physiol*. 2015:169(3):1727–1743. https://doi.org/10.1104/pp.15.01039

Tzin V, Hojo Y, Strickler SR, Bartsch LJ, Archer CM, Ahern KR, Zhou S, Christensen SA, Galis I, Mueller LA, *et al*. Rapid defense responses in maize leaves induced by *Spodoptera exigua* caterpillar feeding. *J Exp Bot*. 2017:68(16):4709–4723. https://doi.org/10.1093/jxb/erx274

Walter M, Chaban C, Schütze K, Batistic O, Weckermann K, Näke C, Blazevic D, Grefen C, Schumacher K, Oecking C, *et al*. Visualization of protein interactions in living plant cells using bimolecular fluorescence complementation. *Plant J*. 2004:40(3):428–438. https://doi.org/10.1111/j.1365-313X.2004.02219.x

Wang Q, Li J, Hu L, Zhang T, Zhang G, Lou Y. OsMPK3 positively regulates the JA signaling pathway and plant resistance to a chewing herbivore in rice. *Plant Cell Rep*. 2013:32(7):1075–1084. https://doi.org/10.1007/s00299-013-1389-2

War AR, Paulraj MG, Ahmad T, Buhroo AA, Hussain B, Ignacimuthu S, Sharma HC. Mechanisms of plant defense against insect herbivores. *Plant Signal Behav*. 2012:7(10):1306–1320. https://doi.org/10.4161/psb.21663

Wasternack C, Hause B. Jasmonates: biosynthesis, perception, signal transduction and action in plant stress response, growth and development. An update to the 2007 review in Annals of Botany. *Ann Bot*. 2013:111(6):1021–1058. https://doi.org/10.1093/aob/mct067

Wouters FC, Blanchette B, Gershenzon J, Vassao DG. Plant defense and herbivore counter-defense: benzoxazinoids and insect herbivores. *Phytochem Rev*. 2016:15(6):1127–1151. https://doi.org/10.1007/s11101-016-9481-1

Wu J, Hettenhausen C, Meldau S, Baldwin IT. Herbivory rapidly activates MAPK signaling in attacked and unattacked leaf regions but not between leaves of *Nicotiana attenuata*. *Plant Cell*. 2007:19(3):1096–1122. https://doi.org/10.1105/tpc.106.049353

Wu XN, Chu L, Xi L, Pertl-Obermeyer H, Li Z, Sklodowski K, Sanchez-Rodriguez C, Obermeyer G, Schulze WX. Sucrose-induced receptor kinase 1 is modulated by an interacting kinase with short extracellular domain. *Mol Cell Proteomics*. 2019:18(8):1556–1571. https://doi.org/10.1074/mcp.RA119.001336

Xie C, Mao X, Huang J, Ding Y, Wu J, Dong S, Kong L, Gao G, Li CY, Wei L. KOBAS 2.0: a web server for annotation and identification of enriched pathways and diseases. *Nucleic Acids Res*. 2011:39(suppl_2):W316–W322. https://doi.org/10.1093/nar/gkr483

Yan Y, Christensen S, Isakeit T, Engelberth J, Meeley R, Hayward A, Emery RJN, Kolomiets MV. Disruption of *OPR7* and *OPR8* reveals the versatile functions of jasmonic acid in maize development and defense. *Plant Cell*. 2012:24(4):1420–1436. https://doi.org/10.1105/tpc.111.094151

Yi R, Shan X. Post-translational modifications: emerging regulators manipulating jasmonate biosynthesis and signaling. *Plant Cell Rep*. 2023:42(2):215–222. https://doi.org/10.1007/s00299-022-02948-w

Yue P, Jiang Z, Sun Q, Wei R, Yin Y, Xie Z, Larkin RM, Ye J, Chai L, Deng X. Jasmonate activates a CsMPK6-CsMYC2 module that regulates the expression of beta-citraurin biosynthetic genes and fruit coloration in orange (*Citrus sinensis*). *Plant Cell*. 2023:35(4):1167–1185. https://doi.org/10.1093/plcell/koac363

Zhai Q, Yan L, Tan D, Chen R, Sun J, Gao L, Dong MQ, Wang Y, Li C. Phosphorylation-coupled proteolysis of the transcription factor MYC2 is important for jasmonate-signaled plant immunity. *PLoS Genet*. 2013:9(4):e1003422. https://doi.org/10.1371/journal.pgen.1003422

Zhang C, Li J, Li S, Ma C, Liu H, Wang L, Qi J, Wu J. ZmMPK6 and ethylene signalling negatively regulate the accumulation of anti-insect metabolites DIMBOA and DIMBOA-Glc in maize inbred line A188. *New Phytol*. 2021:229(4):2273–2287. https://doi.org/10.1111/nph.16974

Zhang M, Zhang S. Mitogen-activated protein kinase cascades in plant signaling. *J Integr Plant Biol*. 2022:64(2):301–341. https://doi.org/10.1111/jipb.13215

Zhu J, Wang WS, Yan DW, Hong LW, Li TT, Gao X, Yang YH, Ren F, LuYT, Yuan TT. CK2 promotes jasmonic acid signaling response by phosphorylating MYC2 in Arabidopsis. *Nucleic Acids Res*. 2023:51(2):619–630. https://doi.org/10.1093/nar/gkac1213